Title: Can leaf net photosynthesis acclimate to rising and more variable temperatures?

Running head: Photosynthetic acclimation to changing temperatures

Giulia Vico[1], Danielle A. Way[2,3], Vaughan Hurry[4], and Stefano Manzoni[5,6]

[1] Department of Crop Production Ecology, Swedish University of Agricultural Sciences (SLU), 750 07 Uppsala, Sweden

[2] Department of Biology, University of Western Ontario, London, ON, Canada N6A 5B7

[3] Nicholas School of the Environment, Duke University, Durham, NC, USA 27708

[4] Umeå Plant Science Centre, Department of Forest Genetics and Plant Physiology, Swedish University of Agricultural Sciences, 901 83 Umeå, Sweden

[5] Department of Physical Geography, Stockholm University, 106 91 Stockholm, Sweden

[6] Bolin Centre for Climate Research, Stockholm University, 106 91 Stockholm, Sweden

Corresponding author:

Giulia Vico, Department of Crop Production Ecology, Swedish University of Agricultural Sciences (SLU)

Address: Ulls väg 16, PO Box 4043, 750 05 Uppsala, Sweden

Email: giulia.vico@slu.se; Phone number: +46 18 67 1418

Keywords: leaf net CO_2 assimilation rate; photosynthesis; thermal acclimation; rising temperatures; climate change; global change; temperature variability; stochastic process

Type of paper: Original Article

Abstract

Under future climates, leaf temperature (T_l) will be higher and more variable. This will affect plant carbon (C) balance because photosynthesis and respiration both respond to short-term (sub-daily) fluctuations in T_l and acclimate in the longer term (days to months). This study asks the question: to what extent can the potential and speed of photosynthetic acclimation buffer leaf C gain from rising and increasingly variable T_l? We quantified how increases in the mean and variability of growth temperature affect leaf performance (mean net CO_2 assimilation rates, A_{net}; its variability; and time under near-optimal photosynthetic conditions), as mediated by thermal acclimation. To this aim, the probability distribution of A_{net} was obtained by combining a probabilistic description of short- and long-term changes in T_l with data on A_{net} responses to these changes, encompassing 75 genera and 111 species, including both C3 and C4 species. Our results show that: i) expected increases in T_l variability will decrease mean A_{net} and increase its variability, whereas the effects of higher mean T_l depend on species and initial T_l; and ii) acclimation reduces the effects of leaf warming, maintaining A_{net} at >80% of its maximum under most thermal regimes.

1. Introduction

Future climate conditions are expected to be warmer, with higher atmospheric CO_2 concentrations, reduced wind speeds and, in many regions, increased plant water stress due to either reduced precipitation or increased atmospheric dryness. Most projections also point to an increase in the variability of air temperature, with enhanced temperature fluctuations within and across days, and more frequent warm extremes (IPCC, 2012). Some of these changes have already been observed, with a number of heat- and drought-related extremes occurring in recent years (e.g., Coumou & Rahmstorf, 2012), along with a general increase in air temperature and decrease in wind speeds (Easterling *et al.*, 2000, McVicar *et al.*, 2012). These shifts in atmospheric conditions affect T_l, with consequences for leaf C dynamics and cascading effects on individual plants, as well as ecosystems and global C cycling.

T_l is determined by the interplay between incoming and emitted radiation and heat exchange via sensible and latent heat exchanges (e.g., Campbell & Norman, 1998, Schymanski, Or & Zwieniecki, 2013). These energy fluxes are controlled by the difference between leaf and air temperature, leaf traits (e.g., leaf size), and transpiration rate. In turn, transpiration rate depends on air temperature and humidity, wind speed, water availability for transpiration, canopy structure and stomatal responses to environmental conditions (including atmospheric CO_2 concentration). Under windy and well-watered conditions (i.e., at or near maximum stomatal opening), T_l generally correlates well with air temperature, although leaves tend to be cooler than air at high air temperature and slightly warmer than air in cooler conditions (Helliker & Richter, 2008, Michaletz *et al.*, 2016). In contrast, in water-limited conditions and under elevated atmospheric CO_2 concentrations, T_l tends to be higher than air temperature due to stomatal closure, which reduces evaporative cooling (Stefan, Frank, Ehsan Eyshi, Henning & Rikard,

2014, Webber *et al.*, 2018). In many ecosystems, T_l and thermal variability are expected to increase under future climate change, due to the joint effects of warmer and more variable air temperatures, higher atmospheric CO_2 concentrations, more intermittent water availability for transpiration, and lower wind speeds (e.g., IPCC, 2013, McVicar *et al.*, 2012, Rahmstorf & Coumou, 2011, Schär *et al.*, 2004). As such, changes in the leaf thermal regime will most likely be of a larger magnitude than those expected for air temperature.

Leaf C fluxes – both photosynthesis and respiration – respond nonlinearly to environmental conditions, including T_l (see, e.g., Bernacchi, Singsaas, Pimentel, Portis & Long, 2001, Medlyn *et al.*, 2002). Therefore, the effects of future changes in air and leaf temperature on plant C balance may alter productivity (Boisvenue & Running, 2006, Reyer *et al.*, 2013, Teskey *et al.*, 2015, Zhao *et al.*, 2017) and eventually lead to shifts in species ranges and local extinctions (Chen, Hill, Ohlemüller, Roy & Thomas, 2011, Loarie *et al.*, 2009). Given the close coupling between T_l and plant productivity, quantifying vegetation responses to climatic changes requires an understanding of leaf-level responses to temperature and thermal fluctuations (Dusenge, Duarte & Way, 2019).

Leaf-level responses to changes in the thermal environment occur over a range of temporal scales. At short time scales (minutes to hours), T_l directly affects many physiological processes, including photosynthesis and respiration (Berry & Bjorkman, 1980, Kruse, Alfarraj, Rennenberg & Adams, 2016, Kruse, Rennenberg & Adams, 2011, Scafaro *et al.*, 2017, Tjoelker, Oleksyn & Reich, 2001, Yamori, Hikosaka & Way, 2014). At low T_l, photosynthetic capacity and respiratory rates increase with temperature as enzyme activity rates increase (Sage & Kubien, 2007, Slot & Kitajima, 2015). Stomata also respond to temperature, both directly (e.g., Peak & Mott, 2011), and indirectly as the result of the increase in vapor pressure deficit that often

accompanies warmer conditions (Lin, Medlyn & Ellsworth, 2012, Oren *et al.*, 1999). As the T_l continues to rise, increases in temperature result in a larger stimulation of respiration and photorespiration than of gross photosynthesis, so that net CO_2 assimilation rate (A_{net}) typically exhibits a concave response to T_l, with an intermediate optimal temperature at which net photosynthesis is maximized (Way & Yamori, 2014).

In turn, the shape of the short-term response of A_{net} to temperature depends on the temperature experienced by the leaf over longer time scales (days to seasons). Recently experienced temperatures drive thermal acclimation, a set of physiological, structural and biochemical adjustments in leaves, affecting every aspect of leaf-atmosphere C exchange (Kattge & Knorr, 2007, Slot & Kitajima, 2015, Smith & Dukes, 2013, Yamori *et al.*, 2014). Thermal acclimation occurs in pre-existing leaves . However, changes in leaf anatomy can also be part of the acclimation process, so that leaves that develop under new thermal environments show greater acclimation than leaves that developed before the temperature change (Armstrong, Logan & Atkin, 2006, Campbell *et al.*, 2007, Slot & Kitajima, 2015, Smith & Dukes, 2017, Way, Oren & Kroner, 2015). Acclimation does not necessarily lead to a higher (or even similar) A_{net} under the new growth conditions (Way & Yamori, 2014). Rather, the net effect of a change in air temperature on plant performance depends on the initial T_l, the extent of the T_l change and, to a certain degree, the species and plant functional type (Atkin & Tjoelker, 2003, Slot & Winter, 2017, Smith & Dukes, 2017, Way & Oren, 2010, Yamori *et al.*, 2014). Thus, thermal acclimation has a potentially marked effect on biosphere-atmosphere C feedbacks, on the long-term mean C balance of ecosystems, and ultimately on atmospheric CO_2 concentrations (Bagley *et al.*, 2015, Heskel *et al.*, 2016, Lombardozzi, Bonan, Smith, Dukes & Fisher, 2015, Smith, Lombardozzi, Tawfik, Bonan & Dukes, 2017, Smith, Malyshev, Shevliakova, Kattge & Dukes, 2016).

Most current efforts to quantify leaf responses to changing temperatures have overlooked how temperature fluctuations that are typical of natural environments impact leaf C fluxes. As such, it is still unclear how temperature fluctuations mediate the short- and long-term thermal responses of A_{net}. Furthermore, few experiments have investigated the speed of acclimation (i.e., how fast existing leaves exposed to a change in thermal regime can acclimate to the new conditions) and if this speed depends on the magnitude of the change in temperature triggering the acclimation response (for some examples, see Battaglia, Beadle & Loughhead, 1996, Slatyer & Ferrar, 1977, Veres & Williams, 1984, Way, Stinziano, Berghoff & Oren, 2017). Hence, it remains uncertain at what timescale thermal acclimation occurs (Rogers *et al.*, 2017, Sendall *et al.*, 2015), particularly when considering natural conditions where temperature fluctuates at multiple time scales, ranging from seconds to days, seasons and decades (Desai, 2014, Medvigy, Wofsy, Munger & Moorcroft, 2010). As a result, the interplay between the extent of thermal acclimation, the timescales over which acclimation occurs, and the magnitude of the fluctuations and long-term changes of T_l is still largely unexplored.

Based on the premise that T_l vary across multiple temporal scales under natural conditions, this study aims to quantify: i) how mean and variability of T_l affect leaf performance; and ii) how these effects are mediated by short- and long-term responses of A_{net} to changes in temperature. To this aim, an extensive dataset on the response of A_{net} to short- and long-term changes in temperature is combined with stochastic models describing the statistical properties of temperature fluctuations and the dynamics of acclimation. The relative importance of the extent and speed of thermal acclimation, and of changes in thermal regime, are quantified and summarized by the long-term mean A_{net}, its variability, and the time spent near optimal conditions for net C uptake. The following specific questions are addressed: i) How is leaf

photosynthetic performance affected by a change in thermal regime? ii) How different are these effects when the change in thermal regime involves an increase in mean temperature, as opposed to a change in the variability of temperature, or a combination of the two? and iii) How do the extent and speed of acclimation affect leaf photosynthetic performance? The results are then used as the basis for recommendations for implementing acclimation responses into dynamic vegetation models.

2. Materials and methods

To answer the above questions, a stochastic description of T_l fluctuations (Section 2.2) was combined with a description of the instantaneous response of A_{net} to T_l (Section 2.1.2), and how such a response is altered by thermal acclimation (Section 2.1.3). The model developments hinge on the patterns emerging from a literature review of the response of A_{net} to short- and long-term changes in T_l (Section 2.1.1). Finally, Section 2.3 develops a statistical characterization of A_{net} based on the stochastic model of T_l, including different descriptions of acclimation. All mathematical symbols are defined in Table S3.

2.1 Short- and long-term responses of net CO_2 assimilation rate (A_{net}) to changes in temperature: Empirical evidence

2.1.1 Literature data collection

To develop and parameterize the model described below, data on the instantaneous response of A_{net} to T_l and how this response changes with growth temperature were collated from the

literature. To best leverage the available data, the focus is on leaf A_{net} as the 'macroscopic' result of the underlying physiological drivers – chiefly, the acclimation of stomatal responses or photosynthetic kinetic constants. Only studies reporting A_{net} measured at different T_l on individual plants grown under at least two different temperature regimes were included in the database. For easy definition of the growth temperature of each plant, T_{growth}, studies conducted under natural (e.g., fluctuating) temperatures were not included. The dataset encompasses results from 77 studies, with 75 genera and 111 species, including trees and C3 and C4 herbaceous species (Table S1 in the Supplementary Information, SI). It significantly extends previous reviews (e.g., that of Yamori *et al.*, 2014), by including 455 short-term responses of A_{net} to T_l. Details on the dataset and the lists of species and literature sources are reported in the SI.

2.1.2 Short-term response

Based on the most common response of A_{net} to short-term changes in T_l (see symbols in Figure 1(c) for an example), a parabolic dependence $A_{net}(T_l)$ was fitted to the observations:

$$A_{net}(T_l) = \begin{cases} -R_{d,min} & T_l < T_{min} \\ k_0 + k_1\, T_l + k_2\, {T_l}^2 & T_{min} \leq T_l \leq T_{max}, \\ -R_{d,max} & T_l > T_{max} \end{cases} \quad (1)$$

where k_i (i=0, 1, 2) are acclimation parameters, $R_{d,min}$ and $R_{d,max}$ are the day respiration rates attained when T_l is below the temperature T_{min} and above the temperature T_{max}, respectively. The parabolic function in Eqn (1) is often employed (see, e.g., Säll & Pettersson, 1994, and subsequent works), because it captures the net effect of different thermal responses of photosynthesis, photorespiration and respiration. Different from previous applications, here the validity of the parabolic dependence is limited to the range $T_{min} \leq T_l \leq T_{max}$. The temperature thresholds T_{min} and T_{max} are defined so that T_{min} is the lowest temperature at which

$k_0 + k_1\, T_l + k_2\, {T_l}^2 = -R_{d,min}$ and T_{max} is the highest temperature at which $k_0 + k_1\, T_l + k_2\, {T_l}^2 = -R_{d,max}$. In other words, A_{net} can be assumed to equal the day respiration rate when T_l is lower than T_{min} and higher than T_{max}. Limiting the validity of the parabolic dependence to the range $T_{min} \leq T_l \leq T_{max}$ avoids the unrealistically low values of A_{net} that would be obtained using the parabolic function without bounds. Note that, for simplicity, no short-term response of A_{net} outside the range $T_{min} \leq T_l \leq T_{max}$ is considered (i.e., $R_{d,min}$ and $R_{d,max}$ are not changing with short-term changes in temperature, but they do acclimate along with A_{opt}; see below). However, for most realistic parameter choices, these conditions are rarely attained, so that the exact definition of $-R_{d,min}$ and $-R_{d,max}$ bears little consequence on the results presented here.

Exploiting the properties of the parabola, the acclimation parameters in Eqn (1), k_i, can be easily linked to those often used to describe the response of A_{net} to short-term fluctuations in T_l (Way & Yamori, 2014): i) the thermal optimum for A_{net}, i.e., T_{opt}; ii) the rate of net CO_2 assimilation at T_{opt} i.e., A_{opt}; and iii) a measure of the temperature range of near-optimal conditions, i.e., $\Delta T_{80\%}$ (the width of the leaf temperature range in which $A_{net} \geq rA_{opt}$, with $r = 0.8$ as in Yamori *et al.* (2014) and Slot and Winter (2017)). T_{opt} corresponds to the position of the vertex of the parabola; A_{opt} is the vertex; and $\Delta T_{80\%}$ can be determined as the difference between the highest and lowest T_l satisfying the equation $k_0 + k_1\, T_l + k_2\, {T_l}^2 = rA_{opt}$. It follows that

$$\begin{aligned} k_0 &= A_{opt} - \frac{4A_{opt}(1-r){T_{opt}}^2}{{\Delta T_{80\%}}^2} \\ k_1 &= \frac{8A_{opt}(1-r)T_{opt}}{{\Delta T_{80\%}}^2} \\ k_2 &= \frac{-4A_{opt}(1-r)}{{\Delta T_{80\%}}^2} \end{aligned} \quad . \qquad (2)$$

The meanings of T_{opt}, A_{opt}, and $\Delta T_{80\%}$ are illustrated graphically in Figure 1(c). Finally, day respiration is assumed to be equal to a fraction of A_{opt} ($R_{d,min} = R_{d,max} = f_R A_{opt}$, with $f_R = 0.1$). T_{min} and T_{max} can thus be readily calculated as a function of T_{opt} , A_{opt}, and $\Delta T_{80\%}$.

2.1.3 Long-term response: leaf thermal acclimation

Leaf gas exchange not only responds to short-term fluctuations in T_l but also acclimates to longer-term changes in the thermal environment. As a result of thermal acclimation, the response of A_{net} to short-term fluctuations in T_l - the function $A_{net}(T_l)$ (Eqn 1) - shifts with growth temperature (Way & Yamori, 2014; see Figure 1(c) for an example). The extent of acclimation was quantified by the difference in the parameters of the parabola (T_{opt}, A_{opt}, and $\Delta T_{80\%}$) between plants of the same species grown under different temperatures within each study.

Most of the data on photosynthetic thermal acclimation are derived from measurements of the response of A_{net} to short-term fluctuations in T_l for plants grown under different growth temperatures for multiple weeks, in most cases focusing on leaves that developed under the growth temperature of interest. Importantly, growth temperature is usually kept stable throughout the experiment (albeit with a day/night cycle) and thus the results provide information on the potential for full thermal acclimation. Hereafter, parameters referring to full acclimation to the growth temperature are denoted by the superscript * (i.e., T^*_{opt}, A^*_{opt}, and $\Delta T^*_{80\%}$ characterize a fully acclimated $A_{net}(T_l)$ response curve).

As discussed in Section 3.1 below, data collated from the literature show that thermal acclimation generally leads to an increase in T^*_{opt} with increased growth temperature. Conversely, the direction of change in $\Delta T^*_{80\%}$ and A^*_{opt} with increasing growth temperature is not

consistent across species. On these bases and to proceed quantitatively, the change of T^*_{opt} with long-term mean T_l, μ_T, is captured via a linear relation (as in Slatyer, 1977b), with slope a_{opt} and intercept b_{opt} determined from the literature data. A linear dependence was chosen because most experiments consider only two growth temperatures, but this choice is corroborated by the few experiments with several temperature treatments (see, e.g., Battaglia *et al.*, 1996, Slatyer, 1977b). Furthermore, while a linear dependence may not be realistic under very large changes in growth temperatures, it holds over ranges exceeding those explored in our analyses. Second, changes in $\Delta T^*_{80\%}$ and A^*_{opt} are considered by assuming that these parameters co-vary with T^*_{opt} (rather than changing with temperature *per se*), following two additional linear relations, i.e., $\Delta T^*_{80\%} = c_{80\%} T^*_{opt} + d_{80\%}$ and $A^*_{opt} = c_{opt} T^*_{opt} + d_{opt}$. The slopes $c_{80\%}$ and c_{opt} and the intercepts $d_{80\%}$ and d_{opt} are determined for each species by interpolation of the fitted acclimation parameters.

Based on our dataset, 156 species- and experiment-specific acclimation responses were obtained, summarizing how the parameters of the parabolic dependence (and their co-variation) change with growth temperature (Figures S1 and S2).

2.2 Leaf temperature and its fluctuations

As the result of the interplay among environmental conditions, plant traits, and leaf-to-atmosphere water fluxes, changes in T_l occur at multiple time scales. There are at least five time scales at which T_l may change: i) within the day, as the result of the (deterministic) diurnal cycle and (stochastic) changes in the leaf energy balance from, e.g., passing clouds and variable wind speed; ii) across several days, due to (stochastic) variation in weather conditions; iii) during the

growing season, following the (deterministic) seasonal cycle; iv) across years, as the result of the (stochastic) inter-annual weather variation; and v) over decades and longer, due to shifts in climatic conditions (e.g., climate change). Here the focus is on the central part of the day and the central part of the growing season, i.e., the periods when light and temperature conditions are most suitable for photosynthesis and hence those most important for plant C uptake. Diurnal and seasonal cycles are therefore neglected, limiting the description to three time scales (sub-daily fluctuations, multi-day weather patterns, and long-term changes in climatic conditions).

To statistically characterize the variability of T_l at these three scales, a minimalist approach is adopted, based on the assumptions that: i) short-term fluctuations are approximately normally distributed; ii) these fluctuations may be temporally correlated due to persistent, multi-day weather patterns; and iii) climatic changes occur at much longer time scales, so they can be captured by changes in the statistical parameters characterizing short-term fluctuations. Combining assumptions i) and ii), the short-term (sub-daily) leaf temperature regime can be described as a correlated (colored) random noise, i.e., the result of the superposition of uncorrelated (white) random Gaussian noise and a temporal autocorrelation (as, e.g., suggested by Benth & Šaltytė-Benth, 2007 for air temperature). The Gaussian white noise captures the short-term fluctuations in temperatures caused by passing clouds or changes in wind speed. The persistence in weather patterns at daily-to-weekly time scale is accounted for by the temporal autocorrelation of temperatures, identified here by the characteristic time scale τ_l. The parameter τ_l describes how rapidly T_l reacts to a short-term random perturbation that forces T_l away from its long-term mean, μ_T. T_l is assumed to revert to μ_T exponentially, with a speed proportional to both $1/\tau_l$ and the difference between the instantaneous value of T_l and its long-term mean μ_T. The details are reported in the SI. This dynamic corresponds to an Ornstein-Uhlenbeck process

(Gardiner, 1990), which results in T_l being normally distributed, with mean μ_T. Its standard deviation, σ_T, depends on the noise size α and characteristic time scale τ_l (see SI2.1).

One example of simulated fluctuations in T_l is shown in Figure 1(a), along with the corresponding probability density function (Figure 1(b); black lines). The sub-daily fluctuations are superimposed on multi-day trends (of time scale τ_l), resulting in alternating warmer and cooler periods. Changes in T_l at long time scales (i.e., years) are described via changes in the long-term mean temperature, μ_T, and the standard deviation of the temperature fluctuations, σ_T (or changes in the noise size α and characteristic time scale τ_l; see SI).

2.3 Short- and long-term responses of net CO_2 assimilation rate (A_{net}) to changes in leaf temperature: Stochastic model

2.3.1 Modelling leaf thermal acclimation

Modelling acclimation under natural thermal environments requires an additional equation to describe how the parameters of the $A_{net}(T_l)$ relation (T_{opt}, A_{opt}, and $\Delta T_{80\%}$) vary in time and how far they are from the fully acclimated values (T^*_{opt}, A^*_{opt}, and $\Delta T^*_{80\%}$). It is assumed that T_{opt} changes over time at a rate proportional to the deviation from its fully acclimated value, T^*_{opt}. Following this assumption, and similar to Dietze (2014) and Säll and Pettersson (1994), the rate of change of T_{opt} is expressed as $\frac{dT_{opt}}{dt} = \left(T^*_{opt} - T_{opt}\right)/\tau_{opt}$. With this formulation, T_{opt} changes exponentially after a step change in temperature, as apparent from the few existing data (Figure S3). The characteristic time scale of thermal acclimation, τ_{opt}, is a measure of the delay inherent in this process, and is defined as the time required for the leaf to react to a change in temperature and reach $1 - e^{-1}$ ≅63% of full acclimation to the new thermal conditions. Note that in this context, T^*_{opt} is the fully acclimated value of T_{opt} – the value that would be reached should T_l remain constant indefinitely. With these assumptions, T_{opt} and the other parameters of the $A_{net}(T_l)$ function follow the dynamics of T_l, but with a delay. The coupled dynamics of T_l and T_{opt} is formally a bi-dimensional Ornstein-Uhlenbeck process. The joint probability distribution of T_l and T_{opt}, $p_{OU}(T_l, T_{opt})$, can be obtained analytically (Gardiner, 1990), as detailed in the SI (Section S2). An example of the resulting dynamics of T_{opt} is plotted in Figure 1(a) (green dashed line). The marginal distributions of T_l and T_{opt} are reported in Figure 1(b) (black and green dashed line respectively). These distributions are needed to calculate the probability density function of A_{net}, as described in Section 2.3.2.

As most of the thermal acclimation data are based on comparisons of plants grown under different but stable temperatures, they cannot be used to determine the speed at which the parameters of the $A_{net}(T_l)$ function reach their fully acclimated values and hence the relaxation constant τ_{opt}. Based on the little available evidence (see Section 3.1), the time for acclimation of τ_{opt} is expected to be on the order of days to weeks. However, given the large uncertainty in this parameter, here three cases are explored in addition to the case of acclimation with delay τ_{opt} just discussed. These three extreme cases are: i) no acclimation (constant T_{opt}); ii) slow acclimation, i.e., the parameters of the function $A_{net}(T_l)$ acclimate to the long-term mean leaf temperature, μ_T (i.e., $T_{opt} = T^*_{opt} = a_{opt}\mu_T + b_{opt}$); and iii) instantaneous acclimation (i.e., $\tau_{opt} \to 0$), where the parameters follow the dynamics of T_l without any delay, reaching their respective fully-acclimated values instantaneously (i.e., $T_{opt} = T^*_{opt} = a_{opt}T_l + b_{opt}$). The instantaneous acclimation scenario is instructive as an extreme case for modeling purposes but it is clearly unrealistic as there are physiological limits to the speed of thermal acclimation. Figure 1(a) shows examples of the dynamics of T_{opt} for each acclimation speed scenario, and how they compare with the dynamics of T_l. The delay in acclimation of T_{opt} results in smoother changes with respect to the case of instantaneous acclimation (compare green dashed and blue dotted lines in Figure 1(a)), while T_{opt} remains constant when acclimating only to the long-term mean temperature or not acclimating at all (red dot-dashed line). It should be noted that, in Figure 1, the case of no acclimation and acclimation to the long-term mean μ_T coincide, because μ_T does not change there.

The dependence of A_{net} on T_l and the effects of the previous history of T_l on the parameters of the function $A_{net}(T_l)$ imply that both short- and longer-term changes in T_l affect the

instantaneous A_{net}. In the model, A_{net} changes as a result of the dynamics of T_l and T_{opt} (and any other parameter of the $A_{net}(T_l)$ function), the potential for acclimation (i.e., the fully acclimated values) and the time scale of the acclimation process (τ_{opt}). Figure 1(d) shows an example of how the joint dynamics of T_l and T_{opt} affect the temporal evolution of A_{net} for different assumptions on the acclimation speed. Faster acclimation results in more variable T_{opt} but, in general, more stable A_{net}.

2.3.2 Probability density function of A_{net} under fluctuating leaf temperatures and resulting leaf performance metrics

Since T_l (and hence T_{opt}) changes randomly, A_{net} must also be treated as a random variable. The probability density function of A_{net} can be determined in two steps. First, by applying the derived distribution technique, the joint probability density function of A_{net} and T_l, $p_{OU}(A_{net}, T_{opt})$, is obtained from the joint probability density function of T_l and T_{opt}, $p_{OU}(T_l, T_{opt})$. Second, the desired probability density function of A_{net}, $p_{OU}(A_{net})$, is retrieved by integrating $p_{OU}(A_{net}, T_{opt})$ over all possible values of T_{opt}. This derivation greatly simplifies when considering the three extreme cases for acclimation speed (no acclimation; acclimation to long-term mean temperature; and instantaneous acclimation; Section 2.3.1), because in these cases T_{opt} is either independent of, or perfectly correlated with, T_l (see SI for details). All the derivations are reported in the SI, along with the analytical formulas of the resulting probability distributions. For illustration, Figure 1(e) compares the probability distributions of A_{net} for the different assumptions of acclimation speed.

Three leaf performance metrics were calculated from the probability distribution of A_{net}: the mean and standard deviation of A_{net} ($\mu_{A_{net}}$ and $\sigma_{A_{net}}$, respectively), as well as the fraction of

time spent at near-optimal conditions (i.e., when $A_{net} \geq 0.8A_{opt}$). Below, we report the mean and standard deviation of A_{net} normalized by the corresponding A_{opt}, to facilitate comparisons across species with different photosynthetic rates and acclimation strategies. The significance of the difference of the performance medians across thermal environments (Section 3.3) was tested using the Mann Whitney test.

3. Results

3.1 Observed acclimation responses: extent and speed

Figure 2(a) summarizes the relative change of the fitted parameters of the $A_{net}(T_l)$ curve (T^*_{opt}, $\Delta T^*_{80\%}$ and A^*_{opt}) for different plant functional types with changing T_{growth}. The most commonly observed acclimation-related change in the $A_{net}(T_l)$ curve is an increase in T^*_{opt} (significant for all functional types). In most experiments, T^*_{opt} does not increase as much as T_{growth}; rather, the mean observed a_{opt} is 0.33 °C °C^{-1} (median: 0.29 °C °C^{-1}) – a value similar to those estimated by Sendall *et al.* (2015), and Yamori *et al.* (2014). An $a_{opt} < 1$ implies that there is a temperature where the optimal and growth temperatures coincide (termed 'preferred temperature' by Slatyer, 1977a). Below the preferred temperature, T^*_{opt} exceeds T_{growth} (and hence an increase in T_l would be beneficial), while above the preferred temperature T_{growth} is higher than T^*_{opt} (and hence a further increase in T_{growth} would be detrimental). Conversely, A^*_{opt} and $\Delta T^*_{80\%}$ do not change consistently across species with increasing growth temperature. Changes in A^*_{opt} and $\Delta T^*_{80\%}$ also appear to be environment-specific, given that observed changes for the same species are not always consistent across experiments.

Figure 2(b) illustrates the covariation of the parameters of the $A_{net}(T_l)$ curve, i.e., the relative change of $\Delta T^*_{80\%}$ and A^*_{opt} with changes in T^*_{opt}. No consistent pattern emerges, with species exhibiting opposite directions of change.

The speed of acclimation was characterized using data from repeated measurements on plants moved from one growth temperature to another (SI1.2). These data suggest that acclimation speed varies between 1 and 14 days (Battaglia *et al.*, 1996, Slatyer & Ferrar, 1977, Veres & Williams, 1984, Way *et al.*, 2017) - clearly shorter than the time required for the development of new tissues under altered growth temperatures. These observations are in agreement with those from natural environments, suggesting that T_{opt} follows the temperature history of the leaf over time windows between 1 to 10 days prior to the observation of T_{opt} (and 1-3 day periods often provide the best match; Gunderson, O'Hara, Campion, Walker & Edwards, 2010, Robakowski, Li & Reich, 2012, Way *et al.*, 2017). Furthermore, at the whole canopy scale, daily net canopy photosynthesis was shown to be correlated with air temperatures at scales from 1 to 30 days in a mixed temperate forested landscape in North America (Desai, 2014).

3.2 Effects of changes in the leaf temperature patterns

Figures 3, 4 and S4 summarize plant performance (mean A_{net}, its standard deviation, and the fraction of time spent under near-optimal conditions, i.e., when $A_{net} > 0.8A^*_{opt}$) for different thermal regimes (i.e., different μ_T and σ_T) and species. The range of thermal regimes investigated here is quite broad by design, despite some indications that the majority of photosynthetic CO_2 assimilation occurs under a small range of leaf temperatures, regardless of latitude and biome (Helliker & Richter, 2008).

An increase in the long-term mean temperature μ_T may have opposite effects on plant performance (Figure 3). Specifically, an increase in μ_T has positive effects (increasing mean A_{net} and reducing the standard deviation of A_{net}) when it brings the leaf nearer to the fully acclimated T^*_{opt} (left portion of each plot in Figure 3), whereas its effect is negative when T_l is pushed further from the thermal optimum (right portions of plots in Figure 3). Conversely, an increase in the variability of T_l (i.e., an increase in σ_T) **always** has a negative effect on plant performance, reducing mean A_{net}, decreasing the fraction of time spent under near-optimal conditions, and increasing the variability of A_{net}.

These general patterns are largely independent of acclimation extent and speed, although the quantitative changes differ (compare rows in Figure 3). When there is no acclimation ((a)-(c)), the range of conditions under which the leaf performs at or near its best is relatively narrow and corresponds to μ_T similar to the (fixed) T^*_{opt}. Any change in the thermal regime has a marked effect on A_{net} and its statistics. For the focus species in Figure 3, *Vicia faba*, thermal acclimation reduces A^*_{opt}, while it increases T^*_{opt} and $\Delta T^*_{80\%}$ (Figure 1c). The latter changes extend the range of conditions under which performance is high and reduce the sensitivity of plant performance to an increase in μ_T. This reduction in the response to changes in the thermal regime is particularly marked in the case of within-season acclimation (here represented by acclimation with a delay of 10 days; Figure 3(g)-(i)). Note that the advantage gained from an even faster acclimation (here represented by the extreme case of instantaneous acclimation; Figure 3(j)-(l)) is rather small and apparent only at high σ_T.

Focusing on the most realistic case (that of delayed acclimation), Figures 4 and S4 explore the performance of six additional species, differing in their acclimation capability and strategies.

Figure 4 summarizes the results for three selected additional species that acclimate to warmer growth temperatures by increasing T^*_{opt} - the most commonly observed response (Figure 2) - while Figure S4 focuses on the less common scenario in which acclimation results in a decrease in T^*_{opt}. Among the species with increasing T^*_{opt} but differing from the acclimation strategy of *Vicia faba, Triticum aestivum* (top row in Figure 4) acclimates by markedly increasing T^*_{opt}, $\Delta T^*_{80\%}$ and A^*_{opt} with growth temperature; *Picea mariana* (middle row) exhibits intermediate acclimation capacity, with increasing T^*_{opt} but decreasing both $\Delta T^*_{80\%}$ and A^*_{opt} under warmer conditions; finally, *Populus balsamifera* (bottom row) has a low acclimation response, consisting of an increase of T^*_{opt} and $\Delta T^*_{80\%}$ but a reduction of A^*_{opt} with temperature (all the parameters are summarized in Table S2). Regardless of the acclimation strategy, changes in the thermal regime (μ_T and σ_T) have qualitatively similar effects to those discussed for *Vicia faba* (Figure 3): increasing σ_T always negatively affects leaf performance, while the effect of increasing μ_T depends on the initial temperature and the response of T_{opt} to a change in temperature. Even if acclimation strategies are different, the overall performance is similarly high within a limited range of thermal conditions around optimal conditions. Similar patterns also emerge in species with a decline in T_{opt} with increasing temperature (e.g. *Phaseolus vulgaris*, *Plantago euryphylla* and *Chenopodium album*; Figure S4). Nevertheless, these species are more sensitive to changes in μ_T then those with increasing T_{opt}, as apparent from the narrowing of the range of conditions where performance is high and stable, regardless of other changes, particularly towards higher μ_T.

3.3 Expected effect of climate change

After considering the responses of selected species to changes in temperature and thermal variability (Figures 3-4, S4), the analyses are extended to the entire dataset to assess the potential effects of a shift in thermal regime, such as that expected under climate change conditions. For each species and average experimental growth temperature μ_T, the performance metrics are determined considering species-specific responses to changes in temperature (Figures S1-S2) and a time scale for acclimation of 10 days. Four thermal regime scenarios are considered (hereafter, the prime denotes the conditions under the shifted thermal regime): i) a control case (μ_T as per the experimental conditions; σ_T=1 °C); ii) an increase in the mean T_l, but unaltered standard deviation with respect to the control ($\mu_T' = \mu_T + 4$ °C; $\sigma_T' = \sigma_T$); iii) an increase in the standard deviation of T_l but unaltered mean T_l ($\sigma_T' = \sigma_T + 2$ °C; $\mu_T' = \mu_T$); and iv) an increase of both mean and standard deviation of T_l ($\mu_T' = \mu_T + 4$ °C; $\sigma_T' = \sigma_T + 2$ °C).

Figure 5 summarizes these results. When pooling all the data together regardless of initial growth temperature (far right bars in Figure 5), plant performance is not significantly affected by a change in the mean growth temperature (compare white and green bars), while an increase in growth temperature variability negatively affects all aspects of plant performance (compare white and blue bars). A simultaneous increase in both mean temperature and temperature variability enhances the variability of A_{net} and reduces the fraction of time when $A_{net} \geq 0.8A_{opt}$ (compare white and red bars in Figure 5(c) and (d) respectively), but has no significant effect on mean A_{net} (Figure 5(b)). While this general pattern holds, some additional significant responses emerge when distinguishing plants based on the lowest μ_T used during the experiments. For example, species subjected to the lowest growth temperatures (far left in Figure 5(b)-(d)) benefit from an increase in μ_T (regardless of whether σ_T is also increased, except for the variability of A_{net}), because under those conditions T_{opt} is generally higher than the initial μ_T. At higher μ_T,

the joint effect of an increase in μ_T and σ_T may instead have negative effects on leaf performance. These results remain unaltered when considered changes in μ_T and σ_T of different (but still realistic) magnitudes and/or larger initial standard deviations, σ_T. Figure 5 thus shows that the patterns detailed for the focal species in Figures 3, 4 and S4 are indeed general.

4. Discussion

4.1 A stochastic framework to account for leaf temperature fluctuations and their interactions with thermal acclimation

Future climate conditions will alter the thermal environment under which leaves operate, increasing the mean and variability of T_l. While leaves can acclimate to shifting thermal regimes, it is currently unclear whether the extent and speed of thermal acclimation of net CO_2 assimilation will be sufficient to buffer predicted increases in the mean and variability of T_l. A novel approach is proposed to interpret the temperature response of A_{net} and thermal acclimation as coupled stochastic processes, thus explicitly accounting for the random nature of T_l. By considering the main temporal scales over which T_l fluctuates and changes (sub-daily, weekly-to-monthly, and inter-annual), the probability density function of A_{net} is obtained. The inclusion of the variability of T_l, and the ensuing partial thermal acclimation, represent a step forward with respect to existing analytical models of photosynthesis and its acclimation (e.g., Säll & Pettersson, 1994). The formulas obtained here permit direct investigation of the role of the different parameters characterizing natural thermal regimes, as well as the short- and long-term responses of leaves to temperature fluctuations, while not requiring computationally heavy simulations. In this sense, our approach is inherently different from previous, simulation-based

studies (e.g., Kattge & Knorr, 2007). Moreover, by characterizing net CO_2 uptake using photosynthetic temperature response curves, the wealth of available data (Way & Yamori, 2014), such as those collated in this work (Table S1), can be exploited. In contrast, less information is available on acclimation of the individual biochemical aspects of photosynthesis and respiration (Kattge & Knorr, 2007, Mercado *et al.*, 2018, Rogers *et al.*, 2017, Stinziano, Way & Bauerle, 2018).

Our approach rests on some simplifications. First, thermal acclimation of net CO_2 assimilation consists of several processes (changes in photosynthetic capacity, photorespiration, and respiration in the light, as well as changes in stomatal conductance; Kattge & Knorr, 2007, Slot & Kitajima, 2015, Yamori *et al.*, 2014). These responses could occur at different time scales, although recent evidence suggests that photosynthetic capacity and respiration may respond at similar time scales (Smith & Dukes, 2018). The response function $A_{net}(T_l)$ (Eqn 1) condenses all these physiological mechanisms via a set of measurable parameters (Eqn 2) and their changes with acclimation. Although not mechanistic, the parabolic shape describes the majority of responses observed, while requiring only three parameters and thus allowing a robust fitting with few data points. However, the model could be modified to accommodate the occasionally observed asymmetric response, such as a rapid decline of A_{net} when T^*_{opt} is exceeded (e.g., Cunningham & Read, 2002). Furthermore, the parabolic response does not account for extreme conditions that have carry-over effects such as permanent damage to foliar enzymes (Berry & Bjorkman, 1980, O'Sullivan *et al.*, 2017). The assumption of linear changes of the parameters with acclimation is motivated by the majority of available studies exploring only two temperatures. This approach has been criticized (Dietze, 2014), as more complex dependences

have been occasionally observed (Slatyer, 1977b). If specific data were available, more realistic dependences could be easily implemented into this framework.

Second, to limit the need for additional parameters and maintain analytical tractability, the effects of diurnal cycles and seasonal changes in T_l are not considered. Sub-optimal conditions when T_l and light availability limit C fixation (shoulder seasons and early/late hours in the day) are quantitatively less relevant for C fixation. Climate change, by altering temperatures, may extend the duration of the thermal conditions most conducive to C fixation, although it could also expose leaves to temperatures above their thermal optimum. Also, by neglecting the diurnal cycle of photosynthesis, some effects of changes in T_l may be underestimated, such as those stemming from the midday decline in photosynthesis and any circadian rhythm in leaf functioning (de Dios *et al.*, 2012, Dietze, 2014).

Finally, our approach does not capture changes in leaf-level gas exchange mediated by growth conditions other than temperature (e.g., water and nutrient availability, atmospheric CO_2 concentration, and vapor pressure deficit). For example, limited water availability may trigger stomatal closure and hence may reduce A_{net}, but reduced evaporative cooling may also increase T_l, thus indirectly affecting net photosynthesis. To capture this feedback, a more detailed description of the leaf-level gas exchange would be needed (Schymanski *et al.*, 2013).

4.2 Role of plant traits on leaf performance and implications under climate change

By incorporating the effects of changes in T_l on photosynthetic performance in a statistical sense, it is shown that an increase in mean T_l may have opposite effects on leaf performance (Figures 3-4), depending on whether this increase brings the leaf nearer to or farther away from its optimal

temperature (Way & Yamori, 2014). Conversely, an increase in the variability of T_l always has a negative effect on leaf performance – an aspect seldom considered in previous works (but see Cerasoli *et al.*, 2014). The negative effect of the variability of T_l has a magnitude comparable to that of a realistic increase in mean temperature (Figures 3-4), underlining the importance of variability in environmental conditions (Frank *et al.*, 2015, Gutschick & BassiriRad, 2003, Medvigy *et al.*, 2010, Reyer *et al.*, 2013). However, our result contrasts with that of Cerasoli *et al.* (2014), where temperature fluctuations had little consequence for leaf gas exchange, most likely due to the extremely wide thermal optimum range of their study species (*Populus deltoides x nigra*).

Based on our model, thermal acclimation significantly reduces the effects of a change in the thermal regime. Thus, acclimation ensures that A_{net} generally remains at or above 80% of the optimal value (Figures 3, 4 and S4), even though the thermal optimum does not perfectly track the thermal regime (Figure 2(a)). This result is in agreement with observations under natural conditions (Cerasoli *et al.*, 2014, Sendall *et al.*, 2015), lending support to our approach. The direction of change of T_{opt} appears to have the largest effect on plant performance outside of the range of near-optimal thermal conditions (Figures 4 and S4). Furthermore, an increase in T_{opt} with growth temperature is more beneficial than a decline in T_{opt} (compare Figure 4 with Figure S4), because matching the thermal optimum with the growth temperature increases leaf performance. These results may partially explain why T^*_{opt} increases with growing temperatures in most species, while changes in $\Delta T^*_{80\%}$ and A^*_{opt} are less consistent (Figure 2).

The speed of acclimation also affects leaf performance. Faster acclimation results in higher and less variable A_{net}, although the marginal advantage decreases at high speeds of acclimation

(Figure 3). Notably, the extreme (and physiologically unrealistic) case of instantaneous acclimation does not confer a major advantage to plant performance (Figure 3, bottom), i.e., the likely biochemical and physiological costs of a faster acclimation rate would likely not be balanced by the increased performance stemming from such high plasticity. The most effective acclimation speed could not be determined, as no information is available on the actual C cost of acclimation and how this cost may change with acclimation speed (Dietze, 2014), although regulating net photosynthesis must be associated with metabolic costs of protein synthesis and degradation, and the maintenance of suitable metabolite pools (Amthor, 2000).

4.3 Implications for dynamic vegetation models

Given the importance of acclimation in modifying plant C gain and modulating vegetation C fluxes, accounting for thermal acclimation has been shown to improve global vegetation models (Arneth, Mercado, Kattge & Booth, 2012, Booth *et al.*, 2012, Dietze, 2014, Huntingford *et al.*, 2017, Mercado *et al.*, 2018, Smith *et al.*, 2016, Stinziano *et al.*, 2018). In spite of its recognized relevance, thermal acclimation of net photosynthesis is still rarely incorporated in these models (Arneth *et al.*, 2012, King, Gunderson, Post, Weston & Wullschleger, 2006, Rogers *et al.*, 2017, Smith & Dukes, 2013; but see Mercado et al., 2018). Furthermore, how and to what level of detail thermal acclimation of photosynthesis and respiration should be parameterized in these models remain open questions (Desai, 2014, Lombardozzi *et al.*, 2015, Medvigy *et al.*, 2010, Rogers *et al.*, 2017, Stinziano *et al.*, 2018), particularly in the light of the large variability in thermal acclimation responses (Figure S1 and S2). While each kinetic parameter acclimates, possibly with different time delays (compare assumptions on respiration and photosynthesis in

Atkin *et al.*, 2008, Kattge & Knorr, 2007), modeling the acclimation of all parameters might be unfeasible, as it would increase computational costs and the needed data for model parameterization is not available. Improvements should thus focus on where the effects on model outcomes can be large. By assessing long-term mean and variation in leaf performance under different levels and speeds of thermal acclimation, this work provides evidence that some features of thermal responses are more relevant than others, thus guiding further model development. Specifically, our results suggest that:

1) Among the parameters defining the shape of the $A_{net}(T_l)$ (Eqn 1), only the optimum temperature for net photosynthesis changes predictably and significantly with growth temperature (Figure 2), whereas variations in the other parameters are inconsistent and less relevant for mean A_{net} (Figure 4, S4). While this work focused on $A_{net}(T_l)$ rather than looking at the responses of individual kinetic parameters, correctly parameterizing the acclimation of the optimal temperatures for photosynthetic parameters emerges as more important than accurately describing other features of the thermal response curves.
2) While neglecting acclimation leads to underestimating mean A_{net} and overestimating its variability away from the optimal temperature (Figure 3 top), the exact speed of acclimation plays a smaller role than the extent of acclimation in determining A_{net} (see Figure 3(d)-(l)), particularly when comparing delayed and instantaneous acclimation. As a first approximation, it could therefore be possible to neglect delays in acclimation in vegetation models and assume that acclimation occurs rapidly enough to be regarded as instantaneous. Although physiologically unrealistic, this approach has the further advantage of reducing the parameters needed, particularly the one describing the speed of acclimation – a rarely investigated trait. Nevertheless, using the previous 30-day averages

as acclimation temperature as done in some models (e.g., Kattge & Knorr, 2007, Smith *et al.*, 2016) might still be adequate, although most acclimation occurs at shorter scales (Figure S3).

3) Acclimation responses are highly species- and potentially environment-specific. Variation across species is larger than across plant functional types (Figures 2, S1 and S2). This range and variability of acclimation responses can be problematic to capture in dynamic vegetation models: using species-averaged responses may not correctly capture the community-level response (Rogers *et al.*, 2017, Stinziano *et al.*, 2018). It is possible (though not demonstrated here) that acclimation responses co-vary with other functional traits that might already be well parameterized.

4.4 Concluding remarks

A stochastic model is proposed to quantify the effects of changes in T_l and fluctuations on the mean and variability of A_{net}, and how these changes are modulated by the extent and speed of thermal acclimation. It is shown that climate change, by increasing not only mean T_l but also its variability, will have detrimental effects on leaf performance, despite acclimation. Indeed, while an increase in mean T_l may have opposite effects on A_{net} depending on growth conditions, an increase in the variability of T_l is always detrimental to leaf C gain, lowering mean A_{net}, increasing its variability, and reducing the time when A_{net} is near its maximum rate. Thermal acclimation is crucial to maintain a high and stable net CO_2 assimilation rate when thermal regimes shift, although the marginal advantage gained by faster acclimation declines with acclimation speed. As such, acclimation of the optimal leaf temperature should be included in

dynamic vegetation models, while acclimation of other photosynthetic traits may be less important for capturing long-term CO_2 assimilation rates.

Acknowledgements

We thank Wataru Yamori for support in the literature search of the acclimation data. GV and VH gratefully acknowledge the partial support of the project "TC4F – Trees and Crops for the Future" funded through the Swedish government's Strategic Research Environment "Sustainable use of Natural Resources". GV was also partially funded by the Swedish Research Council (Vetenskapsrådet) under grant 2016–04910 and the Swedish Research Council for Environment, Agricultural Sciences and Spatial Planning (FORMAS) under grants 942-2016-20001 and 2018-01820. VH and DAW acknowledge collaborative funding from The Swedish Foundation for International Cooperation in Research and higher Education. SM was partly funded by the Bolin Centre for Climate Research and FORMAS under grant 2016-00998. DAW acknowledges support from an NSERC Discovery grant, the Canadian Foundation for Innovation, the Ontario Ministry of Research and Innovation, and an Ontario Early Researcher Award.

Conflicts of interests

The authors declare no conflict of interest.

References

Amthor J.S. (2000) The McCree-de Wit-Penning de Vries-Thornley respiration paradigms: 30 years later. *Annals of Botany*, **86**, 1-20.

Armstrong A.F., Logan D.C. & Atkin O.K. (2006) On the Developmental Dependence of Leaf Respiration: Responses to Short- and Long-Term Changes in Growth Temperature. *American Journal of Botany*, **93**, 1633-1639.

Arneth A., Mercado L., Kattge J. & Booth B.B.B. (2012) Future challenges of representing land-processes in studies on land-atmosphere interactions. *Biogeosciences*, **9**, 3587-3599.

Atkin O.K., Atkinson L.J., Fisher R.A., Campbell C., D., Zaragoza-Castells J., Pitchford J.W., . . . Hurry V. (2008) Using temperature-dependent changes in leaf scaling relationships to quantitatively account for thermal acclimation of respiration in a coupled global climate–vegetation model. *Global Change Biology*, **14**, 2709-2726.

Atkin O.K. & Tjoelker M.G. (2003) Thermal acclimation and the dynamic response of plant respiration to temperature. *Trends in Plant Science*, **8**, 343-351.

Bagley J., Rosenthal D.M., Ruiz-Vera U.M., Siebers M.H., Kumar P., Ort D.R. & Bernacchi C.J. (2015) The influence of photosynthetic acclimation to rising CO_2 and warmer temperatures on leaf and canopy photosynthesis models. *Global Biogeochemical Cycles*, **29**, 194-206.

Battaglia M., Beadle C. & Loughhead S. (1996) Photosynthetic temperature responses of *Eucalyptus globulus* and *Eucalyptus nitens*. *Tree Physiology*, **16**, 81-89.

Benth F.E. & Šaltytė-Benth J. (2007) The volatility of temperature and pricing of weather derivatives. *Quantitative Finance*, **7**, 553-561.

Bernacchi C.J., Singsaas E.L., Pimentel C., Portis A.R. & Long S.P. (2001) Improved temperature response functions for models of Rubisco-limited photosynthesis. *Plant Cell and Environment*, **24**, 253-259.

Berry J. & Bjorkman O. (1980) Photosynthetic response and adaptation to temperature in higher plants. *Annual Review of Plant Physiology and Plant Molecular Biology*, **31**, 491-543.

Boisvenue C. & Running S.W. (2006) Impacts of climate change on natural forest productivity - Evidence since the middle of the 20th century. *Global Change Biology*, **12**, 862-882.

Booth B.B.B., Jones C.D., Collins M., Totterdell I.J., Cox P.M., Sitch S., . . . Lloyd J. (2012) High sensitivity of future global warming to land carbon cycle processes. *Environmental Research Letters*, **7**.

Bunce J.A. (2000) Acclimation of photosynthesis to temperature in eight cool and warm climate herbaceous C3 species: Temperature dependence of parameters of a biochemical photosynthesis model. *Photosynthesis Research*, **63**, 59-67.

Campbell C., Atkinson L., Zaragoza-Castells J., Lundmark M., Atkin O. & Hurry V. (2007) Acclimation of photosynthesis and respiration is asynchronous in response to changes in temperature regardless of plant functional group. *New Phytologist*, **176**, 375-389.

Campbell G.S. & Norman J.M. (1998) *An Introduction to Environmental Biophysics*. (2nd ed.). Springer, New York-Berlin-Heidelberg.

Cerasoli S., Wertin T., McGuire M.A., Rodrigues A., Aubrey D.P., Pereira J.S. & Teskey R.O. (2014) Poplar saplings exposed to recurring temperature shifts of different amplitude exhibit differences in leaf gas exchange and growth despite equal mean temperature. *AoB Plants*, **6**.

Chen I.C., Hill J.K., Ohlemüller R., Roy D.B. & Thomas C.D. (2011) Rapid range shifts of species associated with high levels of climate warming. *Science*, **333**, 1024.

Coumou D. & Rahmstorf S. (2012) A decade of weather extremes. *Nature Clim. Change*, **2**, 491-496.

Cunningham S.C. & Read J. (2002) Comparison of temperate and tropical rainforest tree species: photosynthetic responses to growth temperature. *Oecologia*, **133**, 112-119.

de Dios V.R., Goulden M.L., Ogle K., Richardson A.D., Hollinger D.Y., Davidson E.A., . . . Moreno J.M. (2012) Endogenous circadian regulation of carbon dioxide exchange in terrestrial ecosystems. *Global Change Biology*, **18**, 1956-1970.

Desai A.R. (2014) Influence and predictive capacity of climate anomalies on daily to decadal extremes in canopy photosynthesis. *Photosynthesis Research*, **119**, 31-47.

Dietze M.C. (2014) Gaps in knowledge and data driving uncertainty in models of photosynthesis. *Photosynthesis Research*, **119**, 3-14.

Dusenge M.E., Duarte A.G. & Way D.A. (2019) Plant carbon metabolism and climate change: elevated CO2 and temperature impacts on photosynthesis, photorespiration and respiration. *New Phytologist*, **221**, 32-49.

Easterling D.R., Meehl G.A., Parmesan C., Changnon S.A., Karl T.R. & Mearns L.O. (2000) Climate extremes: Observations, modeling, and impacts. *Science*, **289**, 2068-2074.

Frank D.A., Reichstein M., Bahn M., Thonicke K., Frank D., Mahecha M.D., . . . Zscheischler J. (2015) Effects of climate extremes on the terrestrial carbon cycle: concepts, processes and potential future impacts. *Global Change Biology*, **21**, 2861-2880.

Gardiner G.W. (1990) *Handbook of stochastic methods for physics, chemistry and the natural sciences*. (2nd ed.). Springer, Berlin.

Gunderson C.A., O'Hara K.H., Campion C.M., Walker A.V. & Edwards N.T. (2010) Thermal plasticity of photosynthesis: the role of acclimation in forest responses to a warming climate. *Global Change Biology*, **16**, 2272-2286.

Gutschick V.P. & BassiriRad H. (2003) Extreme events as shaping physiology, ecology, and evolution of plants: toward a unified definition and evaluation of their consequences. *New Phytologist*, **160**, 21-42.

Helliker B.R. & Richter S.L. (2008) Subtropical to boreal convergence of tree-leaf temperatures. *Nature*, **454**, 511-U516.

Heskel M.A., O'Sullivan O.S., Reich P.B., Tjoelker M.G., Weerasinghe L.K., Penillard A., . . . Atkin O.K. (2016) Convergence in the temperature response of leaf respiration across biomes and plant functional types. *Proceedings of the National Academy of Sciences of the United States of America*, **113**, 3832-3837.

Huntingford C., Atkin O.K., Martinez-de la Torre A., Mercado L.M., Heskel M.A., Harper A.B., . . . Malhi Y. (2017) Implications of improved representations of plant respiration in a changing climate. *Nature Communications*, **8**, 1602.

IPCC (2012) *Managing the risks of extreme events and disasters to advance climate change adaptation*. Cambridge University Press.

IPCC (2013) *Climate Change 2013: The physical Science Basis*. Cambridge University Press.

Jensen A.M., Warren J.M., Hanson P.J., Childs J. & Wullschleger S.D. (2015) Needle age and season influence photosynthetic temperature response and total annual carbon uptake in mature *Picea mariana* trees. *Annals of Botany*, **116**, 821-832.

Kattge J. & Knorr W. (2007) Temperature acclimation in a biochemical model of photosynthesis: a reanalysis of data from 36 species. *Plant Cell and Environment*, **30**, 1176-1190.

King A.W., Gunderson C.A., Post W.M., Weston D.J. & Wullschleger S.D. (2006) Atmosphere - Plant respiration in a warmer world. *Science*, **312**, 536-537.

Kruse J., Alfarraj S., Rennenberg H. & Adams M. (2016) A novel mechanistic interpretation of instantaneous temperature responses of leaf net photosynthesis. *Photosynthesis Research*, **129**, 43-58.

Kruse J., Rennenberg H. & Adams M.A. (2011) Steps towards a mechanistic understanding of respiratory temperature responses. *New Phytologist*, **189**, 659-677.

Lin Y.S., Medlyn B.E. & Ellsworth D.S. (2012) Temperature responses of leaf net photosynthesis: the role of component processes. *Tree Physiology*, **32**, 219-231.

Loarie S.R., Duffy P.B., Hamilton H., Asner G.P., Field C.B. & Ackerly D.D. (2009) The velocity of climate change. *Nature*, **462**, 1052-1055.

Lombardozzi D.L., Bonan G.B., Smith N.G., Dukes J.S. & Fisher R.A. (2015) Temperature acclimation of photosynthesis and respiration: A key uncertainty in the carbon cycle-climate feedback. *Geophysical Research Letters*, **42**, 8624-8631.

McVicar T.R., Roderick M.L., Donohue R.J., Li L.T., Van Niel T.G., Thomas A., . . . Dinpashoh Y. (2012) Global review and synthesis of trends in observed terrestrial near-surface wind speeds: Implications for evaporation. *Journal of Hydrology*, **416**, 182-205.

Medlyn B.E., Dreyer E., Ellsworth D., Forstreuter M., Harley P.C., Kirschbaum M.U.F., . . . Loustau D. (2002) Temperature response of parameters of a biochemically based model of photosynthesis. II. A review of experimental data. *Plant, Cell & Environment*, **25**, 1167-1179.

Medvigy D., Wofsy S.C., Munger J.W. & Moorcroft P.R. (2010) Responses of terrestrial ecosystems and carbon budgets to current and future environmental variability. *Proceedings of the National Academy of Sciences of the United States of America*, **107**, 8275-8280.

Mercado L.M., Medlyn B.E., Huntingford C., Oliver R.J., Clark D.B., Sitch S., . . . Cox P.M. (2018) Large sensitivity in land carbon storage due to geographical and temporal variation in the thermal response of photosynthetic capacity. *New Phytologist*, **218**, 1462-1477.

Michaletz S.T., Weiser M.D., McDowell N.G., Zhou J., Kaspari M., Helliker B.R. & Enquist B.J. (2016) The energetic and carbon economic origins of leaf thermoregulation. **2**, 16129.

O'Sullivan O.S., Heskel M.A., Reich P.B., Tjoelker M.G., Weerasinghe L.K., Penillard A., . . . Atkin O.K. (2017) Thermal limits of leaf metabolism across biomes. *Global Change Biology*, **23**, 209-223.

Oren R., Sperry J.S., Katul G.G., Pataki D.E., Ewers B.E., Phillips N. & Schäfer K.V.R. (1999) Survey and synthesis of intra- and interspecific variation in stomatal sensitivity to vapour pressure deficit. *Plant, Cell & Environment*, **22**, 1515-1526.

Peak D. & Mott K.A. (2011) A new, vapour-phase mechanism for stomatal responses to humidity and temperature. *Plant, Cell & Environment*, **34**, 162-178.

Rahmstorf S. & Coumou D. (2011) Increase of extreme events in a warming world. *Proceedings of the National Academy of Sciences*, **108**, 17905-17909.

Reyer C.P.O., Leuzinger S., Rammig A., Wolf A., Bartholomeus R.P., Bonfante A., . . . Pereira M. (2013) A plant's perspective of extremes: terrestrial plant responses to changing climatic variability. *Global Change Biology*, **19**, 75-89.

Robakowski P., Li Y. & Reich P.B. (2012) Local ecotypic and species range-related adaptation influence photosynthetic temperature optima in deciduous broadleaved trees. *Plant Ecology*, **213**, 113-125.

Rogers A., Medlyn B.E., Dukes J.S., Bonan G., von Caemmerer S., Dietze M.C., . . . Zaehle S. (2017) A roadmap for improving the representation of photosynthesis in Earth system models. *New Phytologist*, **213**, 22-42.

Sage R.F. & Kubien D.S. (2007) The temperature response of C3 and C4 photosynthesis. *Plant, Cell & Environment*, **30**, 1086-1106.

Säll T. & Pettersson P. (1994) A model of photosynthetic acclimation as a special case of reaction norms. *Journal of Theoretical Biology*, **166**, 1-8.

Sayed O.H., Emes M.J., Earnshaw M.J. & Butler R.D. (1989) Photosynthetic responses of different varieties of wheat to high temperature: I. Effect of growth temperature on development and photosynthetic performance. *Journal of Experimental Botany*, **40**, 625-631.

Scafaro A.P., Xiang S., Long B.M., Bahar N.H.A., Weerasinghe L.K., Creek D., . . . Atkin O.K. (2017) Strong thermal acclimation of photosynthesis in tropical and temperate wet-forest tree species: the importance of altered Rubisco content. *Global Change Biology*, **23**, 2783-2800.

Schär C., Vidale P.L., Lüthi D., Frei C., Häberli C., Liniger M.A. & Appenzeller C. (2004) The role of increasing temperature variability in European summer heatwaves. *Nature*, **427**, 332.

Schymanski S.J., Or D. & Zwieniecki M. (2013) Stomatal Control and Leaf Thermal and Hydraulic Capacitances under Rapid Environmental Fluctuations. *Plos One*, **8**.

Sendall K.M., Reich P.B., Zhao C.M., Hou J.H., Wei X.R., Stefanski A., . . . Montgomery R.A. (2015) Acclimation of photosynthetic temperature optima of temperate and boreal tree species in response to experimental forest warming. *Global Change Biology*, **21**, 1342-1357.

Silim S.N., Ryan N. & Kubien D.S. (2010) Temperature responses of photosynthesis and respiration in *Populus balsamifera* L.: acclimation versus adaptation. *Photosynthesis Research*, **104**, 19-30.

Slatyer R. (1977a) Altitudinal variation in the photosynthetic characteristics of snow gum, *Eucalyptus pauciflora* Sieb. Ex Spreng. III. Temperature response of material grown in contrasting thermal environments. *Functional Plant Biology*, **4**, 301-312.

Slatyer R. (1977b) Altitudinal variation in the photosynthetic characteristics of snow gum, *Eucalyptus pauciflora* Sieb. ex Spreng. IV. Temperature response of four populations grown at different temperatures. *Functional Plant Biology*, **4**, 583-594.

Slatyer R. & Ferrar P. (1977) Altitudinal variation in the photosynthetic characteristics of snow gum, *Eucalyptus pauciflora* Sieb. ex Spreng. V. Rate of acclimation to an altered growth environment. *Functional Plant Biology*, **4**, 595-609.

Slot M. & Kitajima K. (2015) General patterns of acclimation of leaf respiration to elevated temperatures across biomes and plant types. *Oecologia*, **177**, 885-900.

Slot M. & Winter K. (2017) Photosynthetic acclimation to warming in tropical forest tree seedlings. *Journal of Experimental Botany*, **68**, 2275-2284.

Smith N.G. & Dukes J.S. (2013) Plant respiration and photosynthesis in global-scale models: incorporating acclimation to temperature and CO_2. *Global Change Biology*, **19**, 45-63.
Smith N.G. & Dukes J.S. (2017) Short-term acclimation to warmer temperatures accelerates leaf carbon exchange processes across plant types. *Global Change Biology*, **23**, 4840–4853.
Smith N.G. & Dukes J.S. (2018) Drivers of leaf carbon exchange capacity across biomes at the continental scale. *Ecology*, **99**, 1610-1620.
Smith N.G., Lombardozzi D., Tawfik A., Bonan G. & Dukes J.S. (2017) Biophysical consequences of photosynthetic temperature acclimation for climate. *Journal of Advances in Modeling Earth Systems*, **9**, 536-547.
Smith N.G., Malyshev S.L., Shevliakova E., Kattge J. & Dukes J.S. (2016) Foliar temperature acclimation reduces simulated carbon sensitivity to climate. *Nature Climate Change*, **6**, 407-+.
Stefan S., Frank E., Ehsan Eyshi R., Henning K. & Rikard G. (2014) Impact of heat stress on crop yield—on the importance of considering canopy temperature. *Environmental Research Letters*, **9**, 044012.
Stinziano J.R., Way D.A. & Bauerle W.L. (2018) Improving models of photosynthetic thermal acclimation: Which parameters are most important and how many should be modified? *Global Change Biology*, **24**, 1580-1598.
Teskey R., Wertin T., Bauweraerts I., Ameye M., McGuire M.A. & Steppe K. (2015) Responses of tree species to heat waves and extreme heat events. *Plant Cell and Environment*, **38**, 1699-1712.
Tjoelker M.G., Oleksyn J. & Reich P.B. (2001) Modelling respiration of vegetation: evidence for a general temperature-dependent Q10. *Global Change Biology*, **7**, 223-230.
Veres J.S. & Williams G.J. (1984) Time course of photosynthetic temperature acclimation in *Carex eleocharis* Bailey. *Plant, Cell & Environment*, **7**, 545-547.
Way D.A. & Oren R. (2010) Differential responses to changes in growth temperature between trees from different functional groups and biomes: a review and synthesis of data. *Tree Physiology*, **30**, 669-688.
Way D.A., Oren R. & Kroner J. (2015) The space-time continuum: the effects of elevated CO_2 and temperature on trees and the importance of scaling. *Plant Cell and Environment*.
Way D.A. & Sage R.F. (2008) Thermal acclimation of photosynthesis in black spruce [*Picea mariana* (Mill.) B.S.P.]. *Plant, Cell & Environment*, **31**, 1250-1262.
Way D.A., Stinziano J.R., Berghoff H. & Oren R. (2017) How well do growing season dynamics of photosynthetic capacity correlate with leaf biochemistry and climate fluctuations? *Tree Physiology*, **37**, 879-888.
Way D.A. & Yamori W. (2014) Thermal acclimation of photosynthesis: on the importance of adjusting our definitions and accounting for thermal acclimation of respiration. *Photosynthesis Research*, **119**, 89-100.
Webber H., White J.W., Kimball B.A., Ewert F., Asseng S., Eyshi Rezaei E., . . . Martre P. (2018) Physical robustness of canopy temperature models for crop heat stress simulation across environments and production conditions. *Field Crops Research*, **216**, 75-88.
Yamaguchi D.P., Nakaji T., Hiura T. & Hikosaka K. (2016) Effects of seasonal change and experimental warming on the temperature dependence of photosynthesis in the canopy leaves of Quercus serrata. *Tree Physiology*, **36**, 1283-1295.

Yamori W., Hikosaka K. & Way D.A. (2014) Temperature response of photosynthesis in C-3, C-4, and CAM plants: temperature acclimation and temperature adaptation. *Photosynthesis Research*, **119**, 101-117.

Zhao C., Liu B., Piao S., Wang X., Lobell D.B., Huang Y., . . . Asseng S. (2017) Temperature increase reduces global yields of major crops in four independent estimates. *Proceedings of the National Academy of Sciences of the United States of America*, **114**, 9326-9331.

Figures

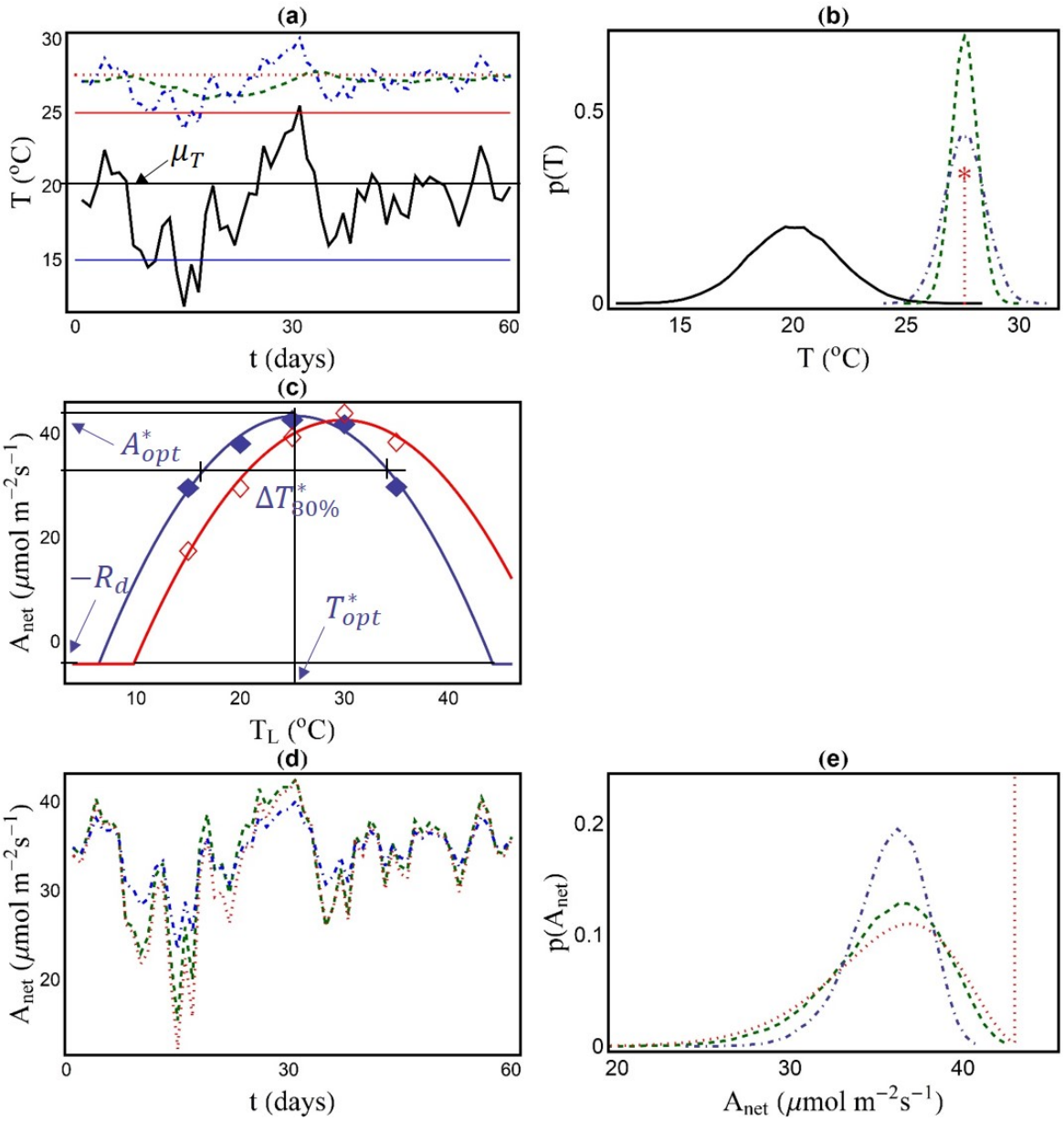

Figure 1 – Summary of the adopted approach. (a) Example of simulated time series of leaf temperature, T_l (solid black line), and the corresponding optimum leaf temperature for photosynthesis, T_{opt} (broken lines), for the different thermal acclimation speeds and (b) corresponding marginal probability density functions of T_l and T_{opt}. (c) Example of the response of A_{net} to short-term fluctuations in leaf temperature, T_l, and how it shifts with

increasing long-term growth temperature (from blue to red) for *Vicia faba* (source of data: Bunce, 2000); closed and open symbols are the observations for plants grown at 15 °C and 25 °C respectively, the solid and dashed lines are the corresponding fitted parabolic response functions $A_{net}(T_l)$ (Eqn (1)). (d) Temporal evolution of the net CO_2 assimilation rate, A_{net}, resulting from the sample trajectories of T_l and T_{opt} in (a) and the temperature response in (c) for the different thermal acclimation speeds. (e) Corresponding probability density functions of A_{net}. In all panels, broken lines refer to different assumptions on the thermal acclimation speed: red dotted lines, no acclimation (which is coincident to acclimation to long-term average leaf temperature μ_T, assuming no changes in μ_T); green dashed lines, acclimation with delay (here, τ_{opt}=10 d); blue dot-dashed lines, instantaneous acclimation. Long-term mean leaf temperature is μ_T =20 °C (as indicated by the horizontal black line in (a)), its standard deviation is σ_T =3 °C, and the characteristic time scale of leaf temperature fluctuations is $\tau_l = 6.7$ d. The simulated time series occasionally reaches the temperatures at which the plants in (c) were grown, as indicated by the crossings of the horizontal thin red and blue lines in (a). The meanings of the acclimation parameters A^*_{opt}, T^*_{opt} and $\Delta T^*_{80\%}$ are graphically depicted in (c) for the lower growth temperature.

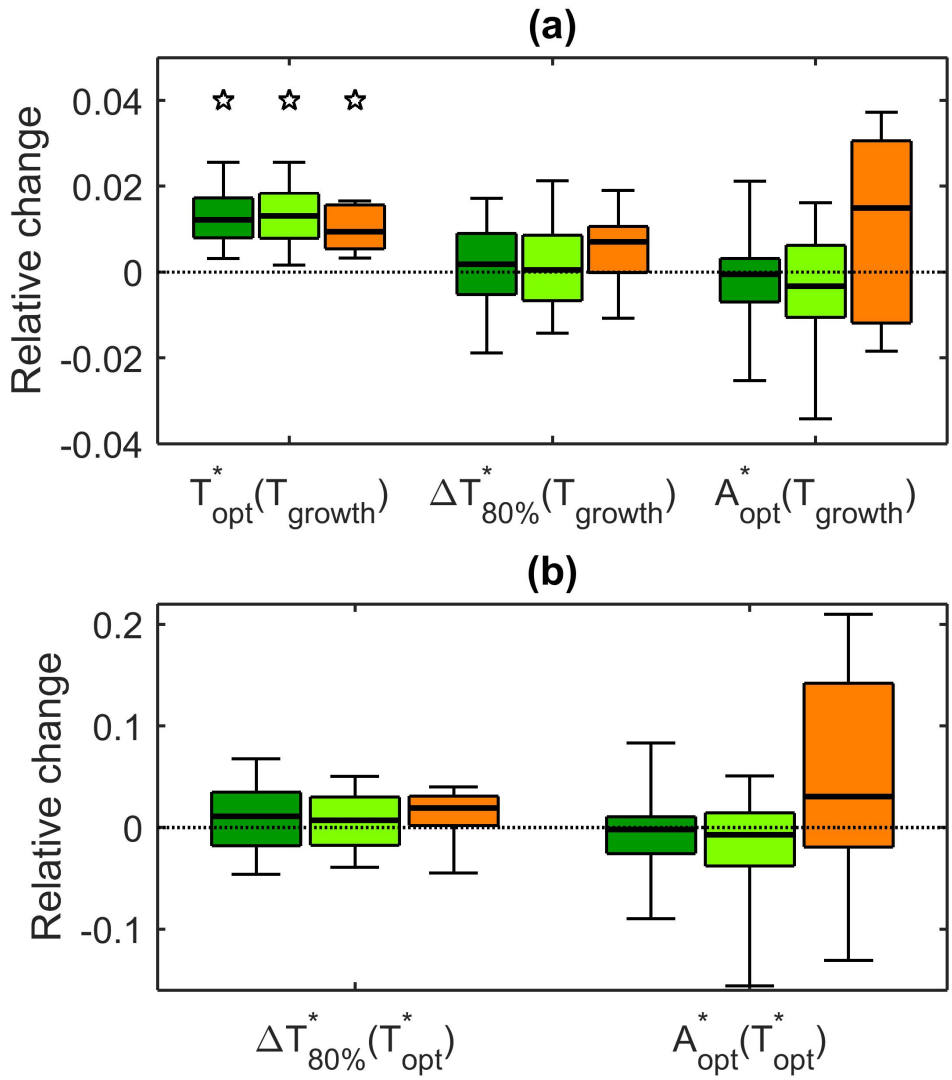

Figure 2 Summary of the observed thermal acclimation responses to an increase in growth temperature. Relative changes of (a) T^*_{opt} (left bar group), $\Delta T^*_{80\%}$ (center bar group) and A^*_{opt} (right bar group) with increasing T_{growth}; and (b) $\Delta T^*_{80\%}$ and A^*_{opt} with a change in T^*_{opt} (i.e., parameter covariation). Colors refer to different functional types: in each group of bars, from left to right, trees are dark green (63 data points), C3 herbs are light green (85 data points), C4 plants are orange (8 data points). In each box, the horizontal thick line is

the median value; boxes extend over the 25th to 75th percentile, whiskers from the 10th to the 90th percentiles. For a generic parameter X, the relative changes are defined in (a) as the slope of the fitted linear function $X(T_{growth})$ and for (b) as the slope of the fitted linear function $X(T^*_{opt})$, in both cases divided by the mean observed X. Bars denoted with star have median values significantly different from zero (at $p<0.01$), based on the Wilcoxon sign test.

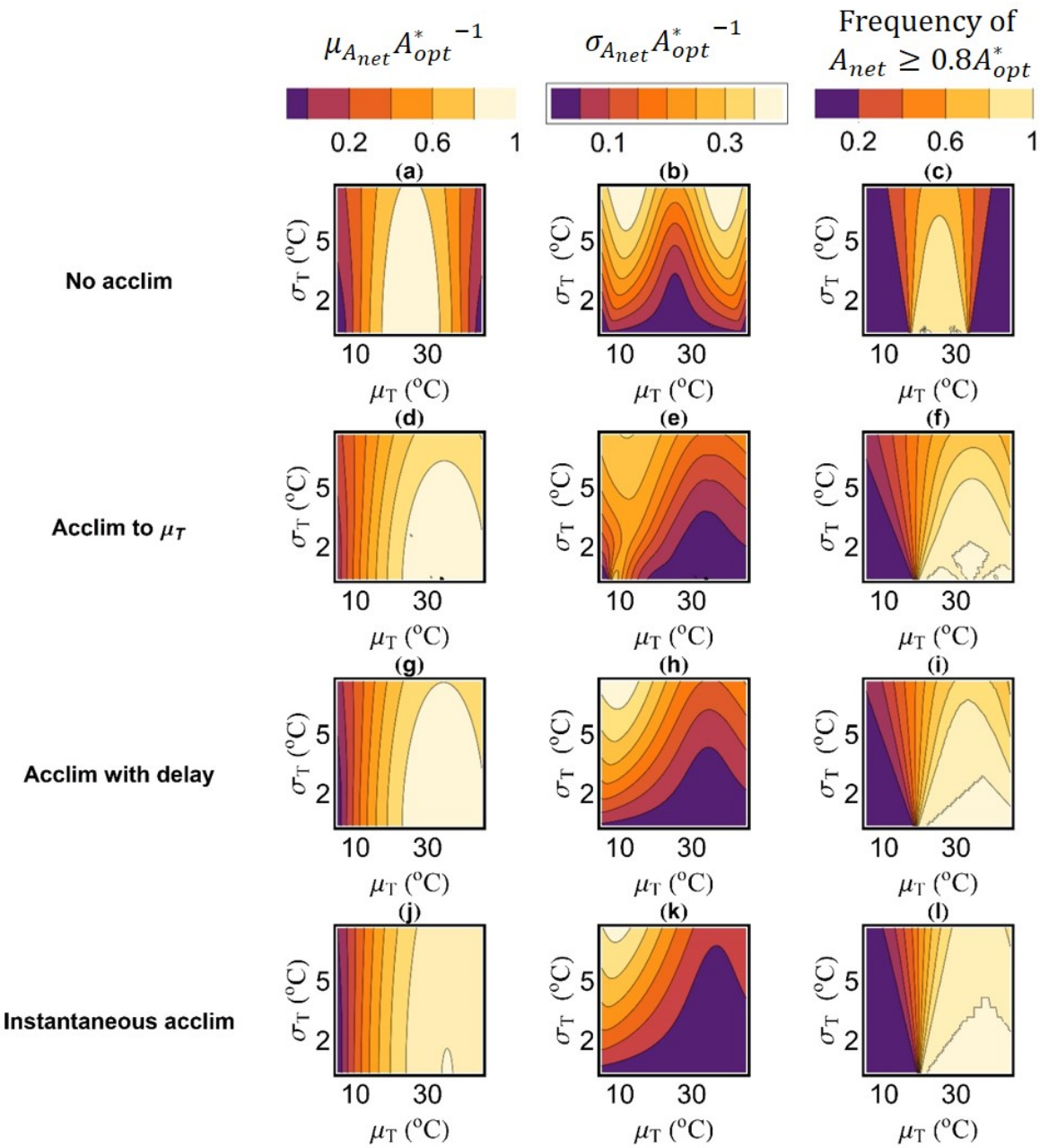

Figure 3 Effects of a shift in the leaf thermal regime on plant performance in *Vicia faba*. The leaf thermal regime is summarized by the long-term average leaf temperature, μ_T (x-axis) and its standard deviation, σ_T (y-axis). Plant performance is summarized by the mean value (left column) and standard deviation (central column) of A_{net}, both normalized by A_{opt} (the acclimated value, when acclimation occurs); and fraction of time spent under optimal or near-optimal conditions (right column). Different assumptions for acclimation

speed are considered: (a)-(c): no acclimation; (d)-(f): acclimation to long-term average leaf temperature, μ_T; (g)-(h): acclimation with a time delay; (j)-(l): instantaneous acclimation. To facilitate the comparison across acclimation speeds, a single color map is used throughout each column, and reported at its bottom. In all cases, data for *Vicia faba* were used to estimate the species-specific model parameters (reported in Table S2). The corresponding fitted $A_{net}(T_l)$ curves are reported in Figure 1(c). In all panels, $\tau_l = 10$ days, so that a change in σ_T (y-axis) results in a change in the size of the noise α (SI, Eqn (1)) as $\alpha = \sigma_T\sqrt{2\tau_l^{-1}}$ (similar patterns would be obtained by altering τ_l instead). For the case of the delayed acclimation ((g)-(i)), $\tau_{opt} = 10$ days.

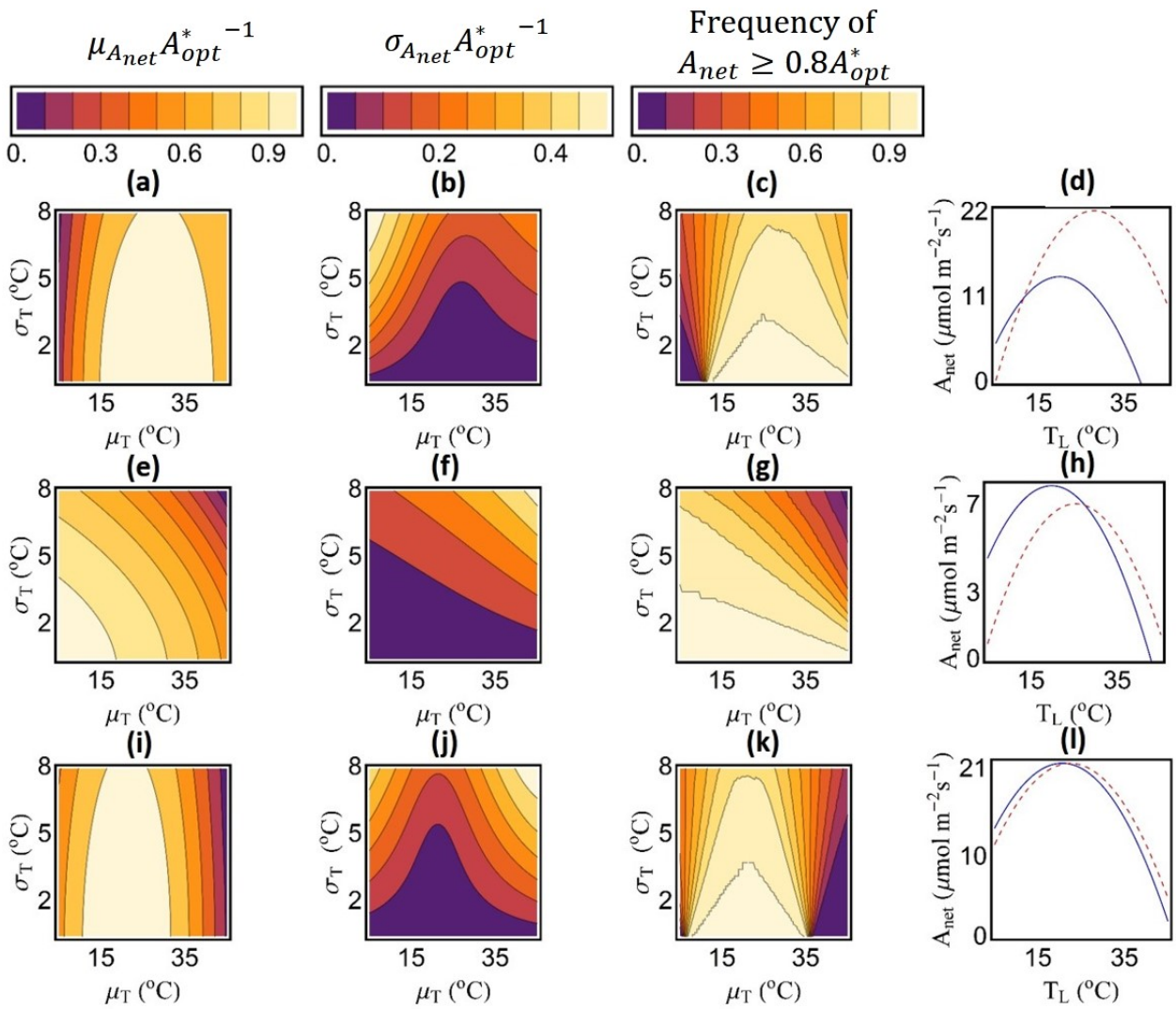

Figure 4 Effects on plant performance of a shift in the leaf thermal regime for three selected species with different acclimation strategies: *Triticum aestivum* (top, panels (a)-(d); acclimation data from Sayed, Emes, Earnshaw & Butler, 1989, cultivar K65), *Picea mariana* (middle, panels (e)-(h); data from Way & Sage, 2008); and *Populus balsamifera* (bottom, panels (i)-(l); data from Silim, Ryan & Kubien, 2010). The leaf thermal regime is summarized by the long-term average leaf temperature, μ_T (x-axis) and its standard deviation, σ_T (y-axis). Plant performance is summarized by the mean (left column) and standard deviation (second column) of A_{net}, both normalized by the species- and

condition-specific A_{opt}; and fraction of time spent under optimal or near-optimal condition (third column). To facilitate the comparison across species, a single color map is used throughout each column, and reported at its bottom. For each species, the $A_{net}(T_l)$ curves for two of the experimental temperatures are reported in the far right column, where blue solid lines refer to the lowest and red dashed lines to the highest temperature considered in each experiment. The species-specific parameters are summarized in Table S2. All the non species-specific parameters are as in Figure 3.

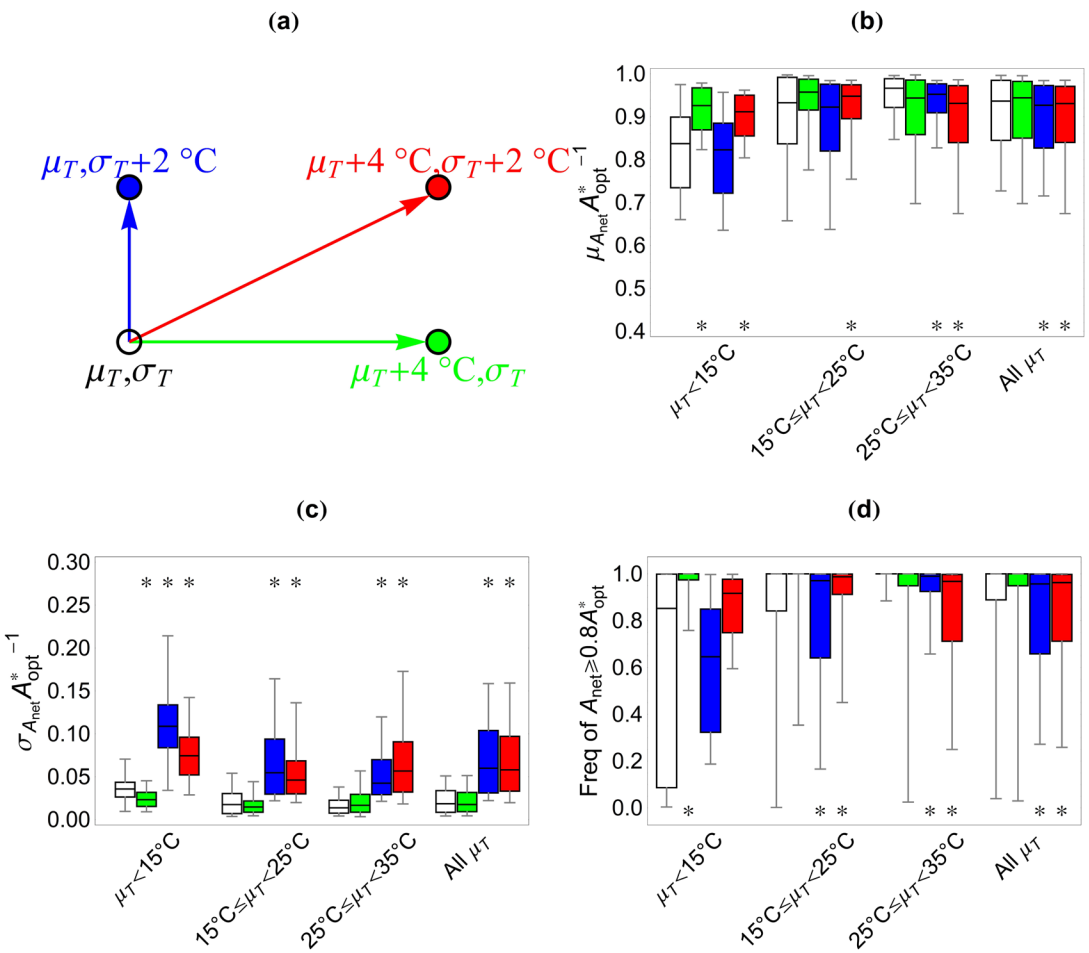

Figure 5 Summary of the effects of selected shifts in the leaf thermal regime on the performance of species included in the acclimation database. (b) Mean values and (c) standard deviations of A_{net}, normalized by the acclimated species-specific A_{opt}, and (d) fraction of time when $A_{net} \geq 0.8A_{opt}$, for each parameter set reported in Figure S1-S2. Results are grouped in three classes of average temperature μ_T, based on the temperature used in each experiment, as specified on the x-axis (from left to right, μ_T lower than 15 °C, between 15 and 25 °C, and between 25 and 35 °C); at the far right, results for all μ_T are grouped together (including some relative to $\mu_T > 35$ °C). In each group, colors represent the four thermal regime scenarios summarized in panel (a): i) in white, the 'control' case (μ_T from the growth conditions; σ_T=1 °C); ii) in green, an increase in mean temperature

($\mu_T' = \mu_T + 4$ °C and $\sigma_T' = \sigma_T$); iii) in blue, an increase in temperature variability ($\mu_T' = \mu_T$ and $\sigma_T' = \sigma_T + 2$ °C); and iv) in red, an increase in mean temperature and temperature variability ($\mu_T' = \mu_T + 4$ °C and $\sigma_T' = \sigma_T + 2$ °C). In (b)-(d), thick horizontal lines are median values, boxes span the 25th-75th percentiles and whiskers extend to the 5th and 95th percentiles. Bars denoted with star have median values significantly different (at p<0.01) from that of the control case (in white) based on the Mann Whitney test.

Can leaf photosynthesis acclimate to rising and more variable temperatures?

Supporting information

Giulia Vico[1], Danielle A. Way[2,3], Vaughan Hurry[4], and Stefano Manzoni[5,6]

[1] Department of Crop Production Ecology, Swedish University of Agricultural Sciences (SLU), 750 07 Uppsala, Sweden

[2] Department of Biology, University of Western Ontario, London, ON, Canada N6A 5B7

[3] Nicholas School of the Environment, Duke University, Durham, NC, USA 27708

[4] Umeå Plant Science Centre, Department of Forest Genetics and Plant Physiology, Swedish University of Agricultural Sciences, 901 83 Umeå, Sweden

[5] Department of Physical Geography, Stockholm University, 106 91 Stockholm, Sweden

[6] Bolin Centre for Climate Research, Stockholm University, 106 91 Stockholm, Sweden

Corresponding author:

Giulia Vico, Department of Crop Production Ecology, Swedish University of Agricultural Sciences (SLU)

Address: Ulls väg 16, PO Box 4043, 750 05 Uppsala, Sweden

Email: giulia.vico@slu.se; Phone number: +46 18 67 1418

SI 1- Observed responses of net CO_2 assimilation rate to leaf temperatures

SI 1.1 Observed short- and long-term response of A_{net} to changes in temperature

Parts of the model developments and its parameterization are based on observed net CO_2 assimilation (A_{net}) responses to short- and long-term changes in temperature. For a robust modelling approach, we collated data available in the literature, reporting the response to short-term changes in temperature for plants acclimated to at least two different growth temperatures for at least one species. Data from plants grown under variable temperatures (e.g., under natural conditions) were not included, even when temperature manipulation was performed, as it would not have been possible to clearly define the growth temperature (necessary for the analyses). The few data on species with CAM photosynthesis were not included in the main dataset: the asynchrony between CO_2 uptake and C fixation by photosynthesis of this metabolic pathway makes the interpretation of the data more complex. When presented in graphical form in the original source, the data were manually digitalized.

The resulting dataset summarizes findings from 77 sources, thus extending by 38% the previous review of this kind of data (Yamori, Hikosaka & Way, 2014). It comprises data from 111 species and 75 genera, including trees, and C3 and C4 herbaceous species. Table S1 reports a summary of the genera, species, and sources of data.

Table S1 Summary of genera and species included in the dataset, and corresponding sources of data

Genus	**Species for which data are available**	**Source(s) of data**
Abutilon	*A. theophrasti*	Bunce (2000), Ziska (2001)
Acer	*A. saccharum*	Gunderson, Norby and Wullschleger (2000)
Agropyron	*A. smithii*	Kemp and Williams (1980), Monson, Robert O. Littlejohn and Williams (1983), Williams (1974)
Amaranthus	*A. retroflexus*	Pearcy, Tumosa and Williams (1981)
Arabidopsis	*A. thaliana*	Bunce (2008), Pons (2012)
Atherosperma	*A. moschatum*	Hill, Read and Busby (1988), Read and Busby (1990)
Athrotaxis	*A. selaginoides*	Read and Busby (1990)
Atriplex	*A. lentiformis; A. glabiriuscola; A. patula; A. rosea; A. sabulosa*	Berry and Bjorkman (1980), Björkman and Pearcy (1971), Pearcy (1977)
Bouteloua	*B. gracilis*	Kemp and Williams (1980), Monson *et al.* (1983), Pittermann and Sage (2000), Williams (1974)
Brassica	*B. napus; B. oleracea; B. rapa*	Bunce (2000), Bunce (2008), Paul, Lawlor and Driscoll (1990)
Buchloe	*B. dactyloides*	Monson *et al.* (1983)
Calamogrostis	*C. canadensis*	Kubien and Sage (2004)
Calophyllum	*C. longifolium*	Slot and Winter (2017)
Carex	*C. eleocharis*	Monson *et al.* (1983), Veres and Williams (1984)
Cenchrus	*C. ciliaris*	Dwyer, Ghannoum, Nicotra and Von Caemmerer (2007)
Ceratopetalum	*C. apetalum*	Hill *et al.* (1988)
Chenopodium	*C. album*	Bunce (2000), Pearcy *et al.* (1981), Sage, Santrucek and Grise (1995)
Colobanthus	*C. quitensis*	Xiong, Mueller and Day (2000)
Corymbia	*C. calophylla*	Aspinwall *et al.* (2017)

Cucumis	*C. sativus*	Yamori, Noguchi, Hikosaka and Terashima (2010)
Deschampsia	*D. antarctica*	Xiong *et al.* (2000)
Dicoria	*D. canescens*	Toft and Pearcy (1982)
Doryphora	*D. sassafras*	Hill *et al.* (1988)
Eucalyptus	*E. argophloia;E. camaldulensis; E. cloeziana; E. incrassata; E. miniata; E. pauciflora; E. regnans; E. saligna; E. sideroxylon*	Ferrar, Slatyer and Vranjic (1989), Ghannoum *et al.* (2010), Ngugi, Hunt, Doley, Ryan and Dart (2003), Slatyer (1977a), Slayter (1977), Warren (2008)
Eucryphia	*E. lucida; E. milliganii; E. moorei*	Hill *et al.* (1988), Read and Busby (1990)
Ficus	*F. insipida*	Slot and Winter (2017)
Flaveria	*F. bidentis*	Dwyer *et al.* (2007)
Geraea	*G. canescens*	Toft and Pearcy (1982)
Geum	*G. rivale; G. urbanum*	Graves and Taylor (1988)
Glycine	*G. max*	Bunce (2000)
Gossypium	*G. hirsutum*	Downton and Slatyer (1972)
Hevea	*H. brasiliensis*	Kositsup *et al.* (2009)
Helianthus	*H. annuus*	Bunce (2000), Paul *et al.* (1990)
Heliotropium	*H. curassavicum*	Mooney (1980)
Hordeum	*H. vulgare*	Bunce (2000)
Lactuca	*L. sativa*	Lorenz and Wiebe (1980)
Lagarostrobos	*L. franklinii*	Read and Busby (1990)
Larix	*L. decidua*	Tranquillini, Havranek and Ecker (1986)
Larrea	*L. divaricata*	Mooney, Björkman and Collatz (1978)
Ledum	*L. groenlandicum*	Smith and Hadley (1974)
Lupinus	*L. arizonicus*	Forseth and Ehleringer (1982)
Lycopersicon	*L. esculentum; L. hirsutum* F1 hybrid*; L. hirsutum; L. solanum*	Bunce (2000), Vallejos and Pearcy (1987)
Malvastrum	*M. rotundifolium*	Forseth and Ehleringer (1982)
Medicago	*M. sativa*	Zaka, Frak, Julier, Gastal and Louarn (2016)

Miscanthus	*Miscanthus x giganteus*	Naidu, Moose, AL-Shoaibi, Raines and Long (2003)
Mucuna	*M. pruriens*	Monson *et al.* (1992)
Muhlenbergia	*M. glomerata*	Kubien and Sage (2004)
Nerium	*N. oleander*	Badger, Björkman and Armond (1982), Björkman, Badger and Armond (1978), Ferrar *et al.* (1989)
Nicotiana	*N. tabacum*	Yamori *et al.* (2010), Yamori and von Caemmerer (2009)
Nothofagus	*N. cf. carrii; N. crenata; N. cf. crenata; N. cunninghamii; N. grandis; N. gunnii; N. moorei; N. perryi; N. pseudoresinosa; N. pullei*	Hill *et al.* (1988), Read (1990), Read and Busby (1990)
Ochroma	*O. pyramidale*	Slot and Winter (2017)
Oryza	*O. sativa*	Nagai and Makino (2009), Yamori *et al.* (2010)
Oxyria	*O. digyna*	Billings, Godfrey, Chabot and Bourque (1971)
Panicum	*P. coloratum*	Dwyer *et al.* (2007)
Pennisetum	*P. setaceum*	Williams and Black (1993)
Phaseolus	*P. vulgaris*	Cowling and Sage (1998)
Phoenix	*P. dactylifera*	Kruse *et al.* (2017)
Phyllocladus	*P. aspleniifolius*	Read and Busby (1990)
Picea	*P. mariana: P. koraiensis; P. likiangensis* (var *rubescens* or var *linzhiensis*)*; P. meyeri; P. sitchensis*	Neilson, Ludlow and Jarvis (1972), Way and Sage (2008a), Way and Sage (2008b), Zhang *et al.* (2015)
Pinus	*P. taeda*	Teskey and Will (1999)
Pisum	*P. sativum*	Haldimann and Feller (2005)
Plantago	*P. asiatica; P. euryphylla ; P. lanceolata; P. major*	Atkin, Scheurwater and Pons (2006), Atkin, Scheurwater and Pons (2007), Ishikawa, Onoda and Hikosaka (2007)
Populus	*P. balsamifera ; P. tremula x P. tremuloides*	Rasulov, Bichele, Hüve, Vislap and Niinemets (2015), Silim, Ryan and Kubien (2010)
Salsola	*S. divaricata*	Gandin, Koteyeva, Voznesenskaya, Edwards and Cousins (2014)

Saxifraga	*S. cernua*	Mawson, Svoboda and Cummins (1986)
Schima	*S. superba*	Sheu and Lin (1999)
Secale	*S. cereale*	Dahal *et al.* (2012), Yamori *et al.* (2010)
Simmondsia	*S. chinensis*	Wardlaw, Begg, Bagnall and Dunstone (1983)
Solanum	*S. tuberosum*	Yamori *et al.* (2010)
Spinacia	*S. oleracea*	Yamori, Noguchi, Hanba and Terashima (2006), Yamori *et al.* (2010), Yamori, Noguchi, Kashino and Terashima (2008), Yamori, Noguchi and Terashima (2005), Yamori, Suzuki, Noguchi, Nakai and Terashima (2006)
Tidestromia	*T. oblongifolia*	Berry and Bjorkman (1980)
Triticosecale	*Triticosecale*	Yamori *et al.* (2010)
Triticum	*T. aestivum*	Nagai and Makino (2009), Sayed, Emes, Earnshaw and Butler (1989), Yamasaki *et al.* (2002), Yamori *et al.* (2010)
Vicia	*V. faba*	Bunce (2000), Yamori *et al.* (2010)
Zea	*Z. mays*	Massacci, Iannelli, Pietrini and Loreto (1995), Naidu *et al.* (2003)

One example of short-term temperature response of net CO_2 assimilation rate, and how it changes with growth temperature, is reported in Figure 1(c) of the main text (symbols). The data collated suggest that similar bell-shaped, symmetric temperature response curves for A_{net} are common, thus supporting the choice of a parabolic response of A_{net} to short-term (sub-daily) changes of leaf temperature T_l. The parabolic dependence $A_{net}(T_l)$ was fitted to the observed response of net CO_2 assimilation rate to short-term changes in T_l, to get T^*_{opt}, $\Delta T^*_{80\%}$ and A^*_{opt}. Being based on only three parameters, the parabolic response can be robustly fitted to most available data, even when relatively few data points were available – a significant advantage with respect to more complex dependences used elsewhere (see, e.g., Cunningham & Read, 2002, Yamori *et al.*, 2014). Note that it is assumed that all the measurements were conducted on fully acclimated leaves (hence, the parameters of the $A_{net}(T_l)$ curve are denoted by *). Indeed 73% of the data included in the dataset refer to leaves newly developed under the new growth temperature, if not to individuals maintained at such temperature throughout their life. The remaining 27% of data refer to leaves developed

at other temperatures, but that were exposed to the new growth temperature for periods that are likely longer than those needed to acclimate (at least according to the few available data on the acclimation speed; see Section SI1.2 below). All the fitted parabolas were checked for realism and robustness. All the convex parabolas (i.e., those with $k_2 < 0$) were removed from the dataset: they were mainly resulting from extremely scattered datapoints or A_{net} not responding to T_l. To avoid excessive extrapolation, those parabolas for which T^*_{opt} was well outside the range of T_l explored in the measurements were also disregarded (specifically, when T^*_{opt} was greater than the maximum measurement T_l plus 10% of the range; or smaller than the minimum measurement T_l minus 10% of the range). The resulting dataset comprises 419 fitted parabolas.

The extent of thermal acclimation was assessed for each species and experiment for which the fitted parabolas were available for at least two growth temperature, by considering the difference in the three fitted parameters between different growth temperatures. Because many experiments explored just two growth temperatures, a linear dependence of the parameters of the parabola on T_{growth} was assumed. The parameters of such linear dependence were obtained by least square fitting of the available data; when more than two growth temperatures were explored in the same experiment, one single line was fitted. Of particular interest is the slope of such lines, i.e., the rate of change of the parameter with changing T_{growth}. The Wilcoxon sign test was used to determine if the median slopes are significantly (at 1%) different from zero.

Figure S1 summarizes the fitted parameters of the $A_{net}(T_l)$ curve (T^*_{opt}, $\Delta T^*_{80\%}$ and A^*_{opt}) and how they change with growth temperature T_{growth}, in each plant functional type. In the left column, lines connect the parameter values (y-axis) observed at different T_{growth} (x-axis) for each species and experiment. The fitted slopes of the parameter-to- T_{growth} lines are summarized in the right column, separated based on the lowest temperature examined in the corresponding experiment (and for all the temperature together; far right bars). The most commonly observed acclimation-related change in the thermal response curve $A_{net}(T_l)$ is an increase in T^*_{opt} with increasing T_{growth}, regardless of functional type and the lowest growth temperature considered in the experiment (Figure S1 top). Conversely, $\Delta T^*_{80\%}$ and A^*_{opt} do not change consistently across species: a large variability emerges, with some species/experiments exhibiting opposite responses to a change in T_{growth}. Hence, it is

possible to conclude that T^*_{opt} is the only parameter that changes consistently with T_{growth} across most species, functional types and initial T_{growth} (Figure S1, right). On these bases and as discussed in the main text, T^*_{opt} is assumed to be the key parameter acclimating to the thermal environment. The median and average change in T^*_{opt} per 1 °C change in T_{growth} emerging from our analyses (Figure S1(b)) are similar to those recently observed by Sendall *et al.* (2015) under natural conditions, but lower than the 0.5 °C °C^{-1} increase obtained by Yamori *et al.* (2014) when considering a smaller dataset and employing third order polynomials.

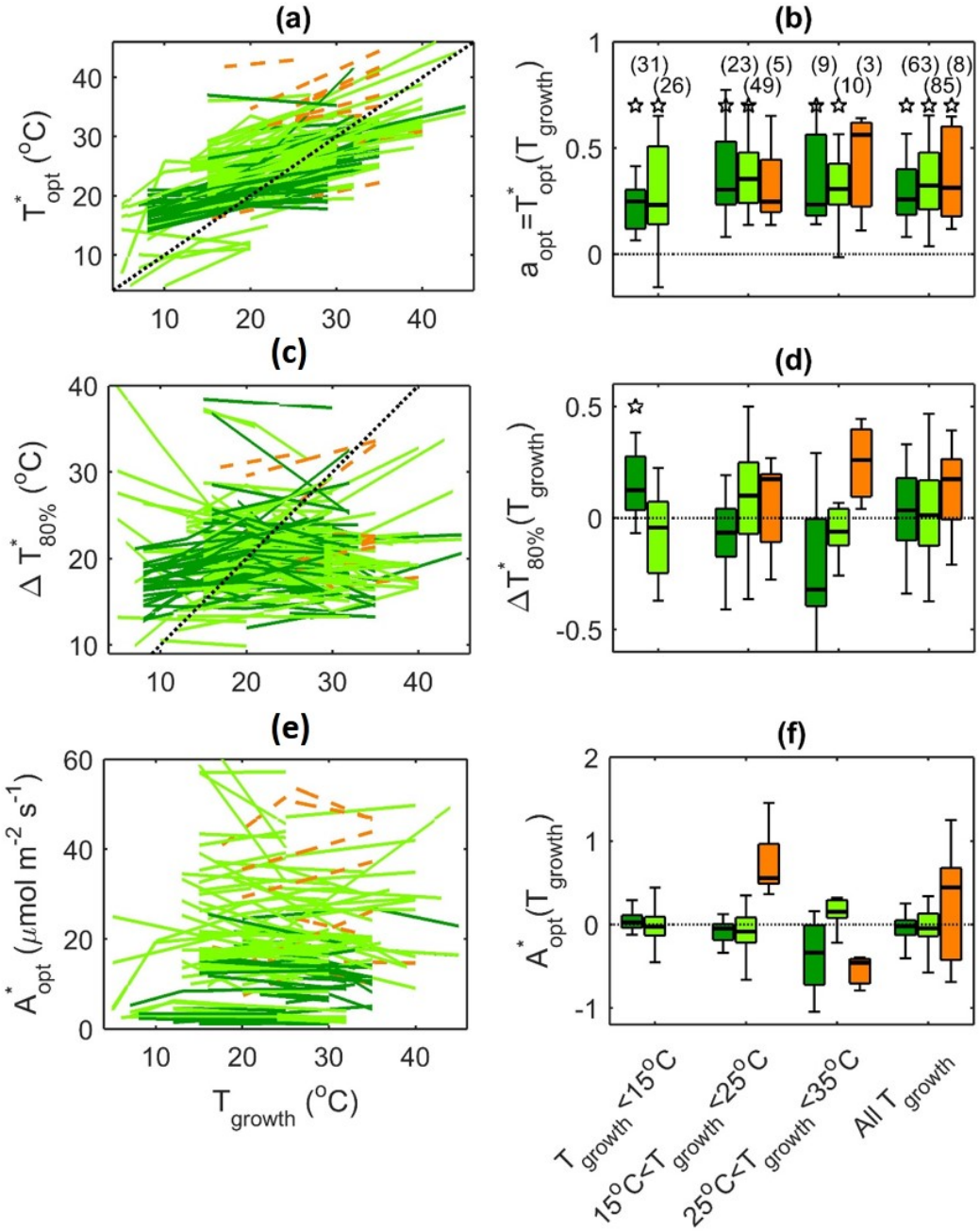

Figure S1 Observed acclimation responses, as summarized by the differences in T^*_{opt} (top), $\Delta T^*_{80\%}$ (middle) and A^*_{opt} (bottom) between plants grown at different temperatures T_{growth}, based on fitting the parabolic response $A_{net}(T_l)$ to the data collated. In the left panels, each line connects the parameters obtained for the same species and variety grown under different temperatures, as indicated on the x-axis. The slopes of such lines are summarized by the box plots in the right panels (horizontal thick lines: median values; boxes extend over the 25th to 75th percentile; whiskers cover the 10th to 90th percentile range). When more than two

growing temperatures were explored in the same experiment, one single line was fitted. In all panels, green solid lines and boxes refer to C3 plants (dark green, trees; light green, herbs); orange dotted lines and boxes to C4 plants. In panels (a) and (c), the dotted black lines are the 1:1 lines. In (b), (d), and (f), the rates of changes are grouped on the basis of the lowest T_{growth} of each experiment or pooled together (far right); the horizontal dotted black lines correspond to slopes equal to zero, i.e., no change in the corresponding parameter with changing T_{growth}; the stars denote medians significantly (at 1%) different from zero, based on the Wilcoxon signed rank test; the sample size is indicated in brackets (the pooled values of the far right include some additional slopes, referring to T_{growth}>35 °C).

The covariation of the parameters of the $A_{net}(T_l)$ curve, and their relative changes, are summarized in Figure S2, showing how $\Delta T^*_{80\%}$ and A^*_{opt} change with T^*_{opt} across functional types and growth temperatures. No clear pattern emerges, suggesting different species may have different acclimation strategies to warming as represented by $\Delta T^*_{80\%}$ and A^*_{opt} (as discussed in Way & Yamori, 2014, Yamori *et al.*, 2014). Yet, a large number of species exhibit some level of covariation of $\Delta T^*_{80\%}$ and A^*_{opt} with T^*_{opt}. These different responses suggest caution when employing assumptions such as that used by Säll and Pettersson (1994), where only T^*_{opt} was assumed to acclimate, while the other parameters were considered 'genetically fixed'. Although this assumption was based on data from *Eucalyptus pauciflora* (Slatyer, 1977b), our dataset suggests this type of response is not universal.

As discussed in the main text, the covariation was accounted for via a linear dependence of $\Delta T^*_{80\%}$ and A^*_{opt} on T^*_{opt}. The slopes of these linear dependence, $c_{80\%}$ and c_{opt}, are summarized in Figure S2 (b) and (c).

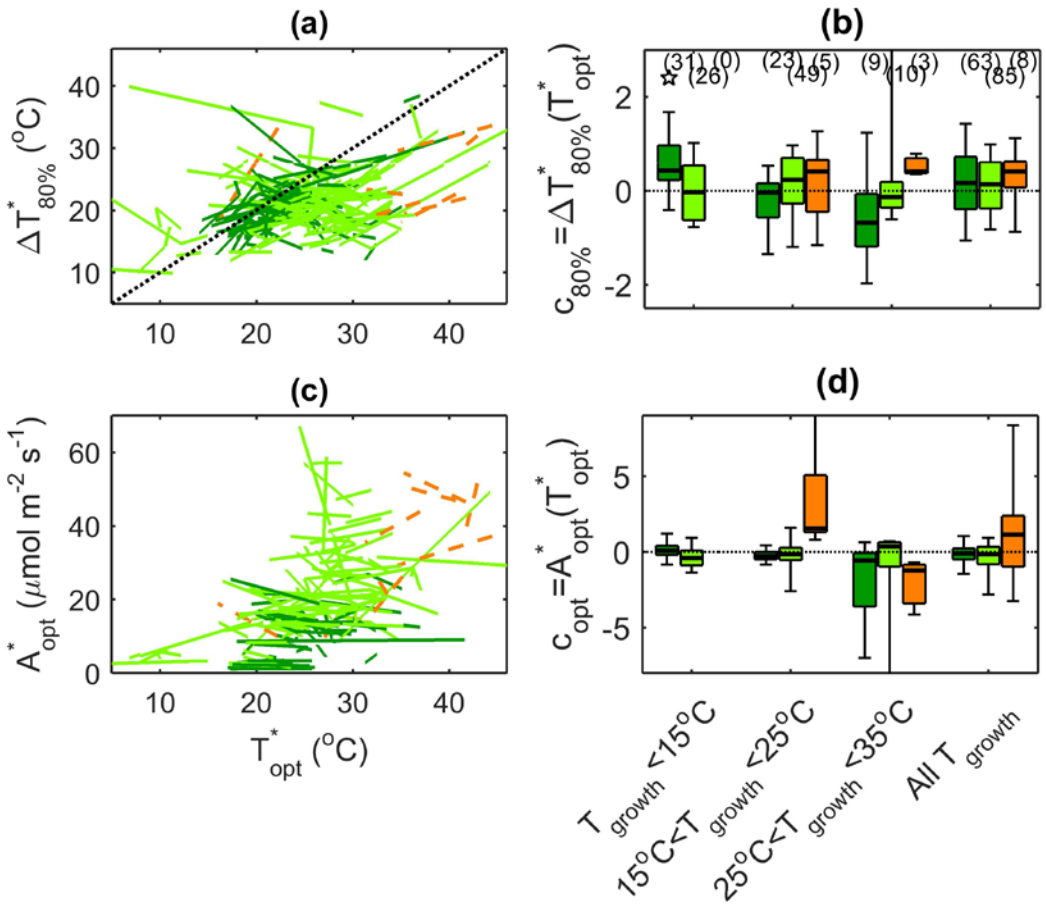

Figure S2 Summary of the observed covariation of the parameters of the fitted parabola $A_{net}(T_l)$: covariation of (a) $\Delta T^*_{80\%}$ and T^*_{opt} and (c) A^*_{opt} and T^*_{opt} (each line connects the parameters obtained for the same species and variety grown under different temperatures). The slopes of such lines are summarized by the box plots in the right panels (horizontal thick lines: median values; boxes extend over the 25th to 75th percentile; whiskers cover the 10th to 90th percentile range). When more than two growing temperatures were explored, one single line was fitted. Green solid lines and boxes refer to C3 plants (dark green, trees; light green, herbs), and orange dotted lines and boxes to C4 plants. In panel (a), the dotted black line is the 1:1 line. In (b) and (d), the slopes are grouped on the basis of the lowest T_{growth} of each experiment or pooled together (far right); the horizontal dotted black lines correspond to slopes equal to zero, i.e., no change in the corresponding parameter with changing T^*_{opt}; the star denotes median significantly (at 1%) different from zero based on the Wilcoxon signed rank test; the sample

size for each box is indicated in brackets (the pooled values of the far right include some additional slopes, referring to T_{growth}>35 °C).

SI1.2 Observed speed of acclimation

The data summarized above cannot provide information on the speed of acclimation, as they focus on the comparison of short-term (sub-daily) responses of A_{net} to temperature fluctuations in leaves from individuals grown under different (but otherwise constant) temperatures. Quantifying the speed of acclimation requires specific observations. One approach is to repeat the measurements on plants moved from one growing temperature to another, at different times after exposure to the new growth temperature (for some examples, see, e.g., Battaglia, Beadle & Loughhead, 1996, Nobel & Hartsock, 1981, Slatyer & Ferrar, 1977, Veres & Williams, 1984). An alternative approach is based on correlating leaf C exchange rates to time-lagged temperatures in natural conditions (Battaglia *et al.*, 1996, Sendall *et al.*, 2015, Way, Stinziano, Berghoff & Oren, 2017). Here only the first type of data are considered, because they are easier to interpret within our modelling approach.

Figure S3 summarizes the temporal trajectories of T_{opt} (and in one case also A_{opt} and $\Delta T_{80\%}$) from the few studies reporting this type of data (including data for a CAM species, to maximize the data availability). To facilitate the comparison across species and studies, all the values are normalized with respect to those measured at the time of the change in thermal regime. The available data suggest that acclimation in existing leaves occurs over time periods of 1-14 days (Battaglia *et al.*, 1996, Slatyer & Ferrar, 1977, Veres & Williams, 1984, Way *et al.*, 2017). It should be noted that the results of Nobel and Hartsock (1981) for CAM species point to different delays depending on the direction of the temperature change. Nevertheless, due to the limited evidence, delays are here assumed to be independent of the direction of temperature change.

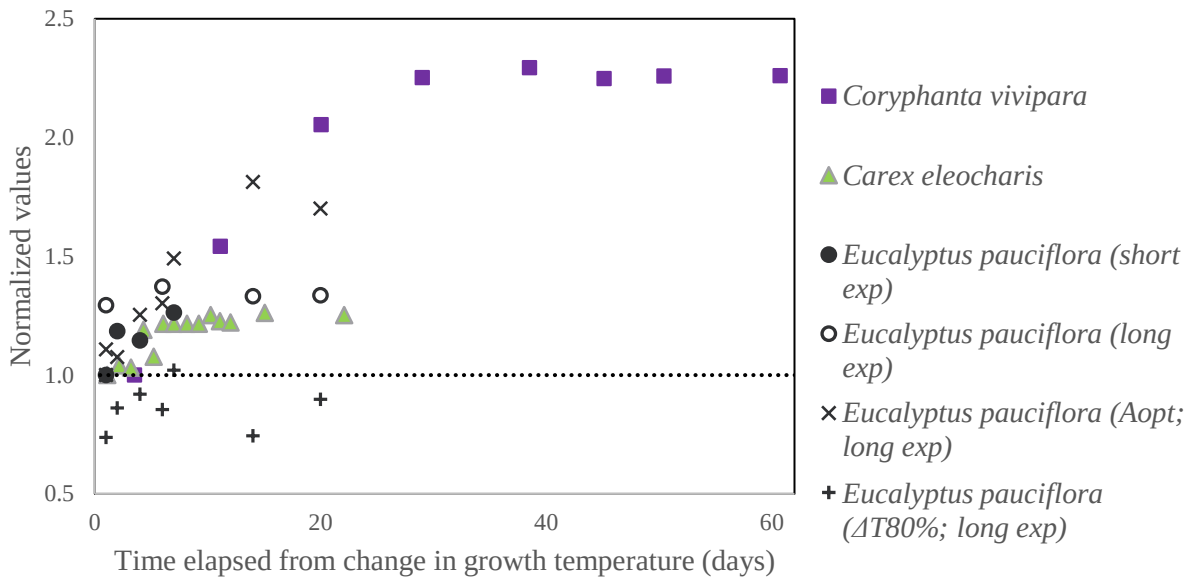

Figure S3 Normalized observed changes in T_{opt} (shapes), A_{opt} (x) and $\Delta T_{80\%}$ (plus sign), as a function of time (days) elapsed from the change in temperature regime. Data refer to *Coryphanta vivipara* (violet squares; Nobel & Hartsock, 1981), *Carex eleocharis* (light green triangles; Veres & Williams, 1984), and *Eucalyptus pauciflora* (dark green symbols; closed symbols refer to the short experiment, open symbols to the long experiment; Slatyer & Ferrar, 1977). To facilitate the comparison across parameters and species, all values were normalized with respect to their value at the time of the change in the thermal regime (i.e., $T_{opt}(t = 0)$ and $A_{opt}(t = 0)$). The horizontal dashed line corresponds to no change in time.

SI1.3 Model parameterization

The information summarized in Figure S1-S3 was used for the species- and experiment-specific parameterization of the A_{net} response to short- and long-term changes in temperature. Specifically, the T^*_{opt}, A^*_{opt} and $\Delta T^*_{80\%}$ summarized in Figure S1 (left column) provide the parameters of the $A_{net}(T_l)$ curve for set T_{growth}. The slopes and intercepts emerging from the lines in Figure S1(a) correspond to the parameters a_{opt} and b_{opt} respectively, employed to characterize the response of the optimum temperature for net CO_2 assimilation at full acclimation, T^*_{opt}, to the average growth temperature, T_{growth} (Section 2.1 in the main text). The slopes and intercepts of the lines in Figure S2 (left) are used to infer the species-specific parameters $c_{80\%}$ and $d_{80\%}$ (and c_{opt} and d_{opt}), which account for the covariation of $\Delta T^*_{80\%}$ (and A^*_{opt}) with T^*_{opt}. Note that it is assumed that the long-term mean leaf temperature, μ_T, can be considered substantially equal to the constant diurnal air temperature T_{growth} set in each experiment. This is realistic, given the artificial conditions typical of these experiments (performed in greenhouses or growth chambers).

Because of the large variability in response to short-term changes in temperature and in the co-variation of the associated parameters, seven species are compared (Figure 3 and 4 in the main text; Figure S4) and then general conclusions are drawn considering the entire database (Figure 5 in the main text). The parameters of the seven focal species are summarized in Table S2.

Table S2 Species-specific parameters used in Figure 3 and 4 in the main text and Figure S4. Values in parenthesis refer to the highest growth temperature explored in the study.

	Vicia faba	*Triticum aestivum*	*Picea mariana*	*Populus balsamifera*	*Phaseolus vulgaris*	*Plantago euryphylla*	*Chenopo-dium album*
Source of data	Bunce (2000)	Sayed *et al.* (1989), Cultivar K65	Way and Sage (2008b)	Silim *et al.* (2010)	Cowling and Sage (1998)	Atkin *et al.* (2006)	Bunce (2000)
Figure	Fig. 3	Fig. 4 (top)	Fig. 4 (middle)	Fig. 4 (bottom)	Fig. S4 (top)	Fig. S4 (middle)	Fig. S4 (bottom)
T_{growth} (°C)	15 (25)	13 (30)	24 (30)	19 (27)	25 (36)	13 (27)	15 (25)
A^*_{opt} (µmol m^{-2} s^{-1})	43.4 (42.6)	13.5 (22.1)	7.85(7.03)	21.6 (21.6)	15.4 (19.1)	15.1 (8.71)	58.7 (32.7)
T^*_{opt} (°C)	25.3 (29.8)	20.0 (28.0)	19.8 (25.3)	20.6 (22.5)	29.5 (29.3)	26.1 (21.1)	27.3 (26.9)
$\Delta T^*_{80\%}$ (°C)	16.1 (17.1)	16.8 (20.7)	20.5 (19.2)	22.8 (22.8)	20.1 (19.3)	24.2 (21.8)	16.7 (18.7)
a_{opt} (°C °C^{-1})	0.453	0.472	0.924	0.233	-0.011	-0.359	-0.035
b_{opt} (°C)	18.5	13.7	-2.38	16.2	29.7	30.4	27.8
$c_{80\%}$ (°C °C^{-1})	0.220	0.478	-0.238	-0.001	6.73	0.342	-5.61
$d_{80\%}$ (°C)	10.6	7.29	25.2	22.8	-178	15.7	169
c_{opt} (µmol m^{-2} s^{-1} °C^{-1})	-0.174	1.06	-0.148	-0.014	-31.6	1.37	74.1
d_{opt} (µmol m^{-2} s^{-1})	47.8	-7.75	10.77	21.9	945	-20.9	1963

SI2- Mathematical developments

This appendix explains the technical aspects of the model describing the dynamics of T_l and that of the parameters of the short-term response to changes in T_l, as well as the derivation of the probability density functions (pdf) of T_l, T_{opt}, and A_{net}. Knowledge of the pdf of A_{net} allows determining the leaf performance proxies by integration. All the symbols are summarized in Table S3.

Although the specifics of the mathematical derivations depend on the acclimation speed assumed (see below), the following steps are needed in all cases.

1) Assumptions on the dynamics of T_l and T_{opt} are employed to derive the probability density function of T_l or the joint probability density function of T_l and T_{opt}, if also T_{opt} changes (Section S2.1 and S2.3, respectively).
2) Knowledge of the net CO_2 assimilation response to short-term fluctuations (Eqn 1 in the main text) and of the pdf of T_l (or T_l and T_{opt}) allows the determination of the pdf of A_{net}, employing the derived distribution technique (Kottegoda & Rosso, 1998; Sections S2.2 and S2.3). This approach exploits the conservation of probability for dependent and independent variables linked by a functional relation. This step can be performed analytically only when the parabolic dependence $A_{net}(T_l)$ can be analytically inverted. This is the case for species that do not alter their A_{opt} during acclimation, i.e., in which only T_{opt} and/or $\Delta T_{80\%}$ change. To avoid excessively cumbersome expressions, the analytical solutions are reported only for the case of the sole T_{opt} changing (i.e., $\Delta T_{80\%}$ and A_{opt} are constant). When also A_{opt} and $\Delta T_{80\%}$ acclimate, the derived distribution can be obtained via a Monte Carlo approach (see, e.g., Lemieux, 2009).
3) The last step is the quantification of leaf performance metrics from the pdf of A_{net}. Here three metrics are employed: the mean and standard deviation of A_{net} ($\mu_{A_{net}}$ and $\sigma_{A_{net}}$ respectively), and the fraction of time spent under near-optimal conditions (i.e., $P\left(A_{net} \geq rA^*_{opt}\right)$, with $r = 0.8$). These metrics can be obtained directly through integration of $p(A_{net})$. Due to the complexity of $p(A_{net})$, this final integration must be conducted numerically in all cases, i.e., also when $p(A_{net})$ is available as a closed formula.

Table S4 summarizes the cases considered here and the steps to achieve the pdf of A_{net}.

Table S3 Summary of the mathematical symbols used in this paper.

Symbol	Description
A_{net}	Net CO_2 assimilation rate
A_{opt}	Net CO_2 assimilation rate at T_{opt} (i.e., parabola vertex)
A^*_{opt}	Net CO_2 assimilation rate at T_{opt} (i.e., parabola vertex) for fully acclimated leaves
a_{opt}	Slope of the linear relation describing the acclimation of T^*_{opt} with leaf temperature ($T^*_{opt} = a_{opt}T_l + b_{opt}$)
b_{opt}	Intercept of the linear relation describing the acclimation of T^*_{opt} with leaf temperature ($T^*_{opt} = a_{opt}T_l + b_{opt}$)
$c_{80\%}$	Slope of the linear relation linking $\Delta T^*_{80\%}$ to T^*_{opt} ($\Delta T^*_{80\%} = c_{80\%}T^*_{opt} + d_{80\%}$)
c_{opt}	Slope of the linear relation linking A^*_{opt} to T^*_{opt} ($A^*_{opt} = c_{opt}T^*_{opt} + d_{opt}$)
$d_{80\%}$	Intercept of the linear relation linking $\Delta T^*_{80\%}$ to T^*_{opt} ($\Delta T^*_{80\%} = c_{80\%}T^*_{opt} + d_{80\%}$)
d_{opt}	Intercept of the linear relation linking A^*_{opt} to T^*_{opt} ($A^*_{opt} = c_{opt}T^*_{opt} + d_{opt}$)
f_R	Ratio of day respiration ($R_{d,min}$ and $R_{d,max}$) to A_{opt} ($f_R = 0.1$)
k_i (i=0, 1, 2)	Parameters of the parabolic dependence $A_{net}(T_l)$, linked to A^*_{opt}, T^*_{opt} and $\Delta T^*_{80\%}$ as per Eqn (2) in the main text
J	Jacobian of the transformation of variables (from T_l and T_{opt} to $\widetilde{T}_l$ and $\widetilde{T}_{opt}$)
$p(T_l)$	Steady-state probability density function of T_l
$p_{inst,c}(A_{net})$	Probability density function of A_{net} for the case of instantaneous acclimation (continuous part)
$p_{long,c}(A_{net})$	Probability density function of A_{net} for the case of no acclimation or acclimation to the long-term mean temperature (continuous part)
$p_{OU}(\widetilde{T}_l, \widetilde{T}_{opt})$	Joint probability density function of the shifted variables $\widetilde{T}_l$ and $\widetilde{T}_{opt}$ for the bi-dimensional Ornstein-Uhlenbeck process (i.e., acclimation with delay)
$p_{OU}(T_l, T_{opt})$	Joint probability density function of T_l and T_{opt} for the bi-dimensional Ornstein-Uhlenbeck process (i.e., acclimation with delay)
$p_{OU}(A_{net}, T_{opt})$	Joint probability density function of A_{net} and T_{opt} for the bi-dimensional Ornstein-Uhlenbeck process (i.e., acclimation with delay) with only T_{opt} acclimating
$p_{OU,c}(A_{net})$	Continuous part of the marginal probability density function of A_{net} for the bi-dimensional Ornstein-Uhlenbeck process (i.e., acclimation with delay) with only T_{opt} acclimating
$p_{OU,T_{opt}\|T_l}(T_{opt}\|T_l)$	Conditional probability density function of T_{opt} given T_l for the bi-dimensional Ornstein-Uhlenbeck process (i.e., acclimation with delay)
$p_{OU,T_l}(T_l)$	Marginal probability distribution of T_l for the bi-dimensional Ornstein-Uhlenbeck process (i.e., acclimation with delay)
$P_{OU,T_{opt}\|T_l}(T_{opt}\|T_l)$	Cumulative conditional probability density function of T_{opt} given T_l for the bi-dimensional Ornstein-Uhlenbeck process (i.e., acclimation with delay)
$P_{OU,T_l}(T_l)$	Cumulative marginal probability distribution of T_l for the bi-dimensional Ornstein-Uhlenbeck process (i.e., acclimation with delay)

$p_{0,low,inst}$, $p_{0,high,inst}$	Atoms of probability for the case of instantaneous acclimation (located in $T_{min,inst}$ and $T_{max,inst}$ respectively)
$p_{0,low,long}$, $p_{0,high,long}$	Atoms of probability for the case of no acclimation or acclimation to the long-term mean temperature (located in $T_{min,long}$ and $T_{max,long}$ respectively)
$p_{0,low,OU}$, $p_{0,high,OU}$	Atoms of probability for the case of the bi-dimensional Ornstein-Uhlenbeck process (i.e., acclimation with delay) with only T_{opt} acclimating (located in $T_{min,OU}$ and $T_{max,OU}$ respectively)
r	Fraction of A_{opt} above which net CO_2 assimilation rate is considered near optimal (r=0.8)
$R_{d,min}$, $R_{d,max}$	Day respiration rates attained at T_{min} and T_{max}, respectively
T_l	Leaf temperature
$\widetilde{T_l}$	Shifted leaf temperature ($\widetilde{T_l} = T_l - \mu_T$)
T_{min}, T_{max}	Temperatures below and above which A_{net} is assumed to be constant and equal to $-R_{d,min}$ and $-R_{d,max}$ respectively
T_{opt}	Optimal temperature for photosynthesis (i.e., position of the parabola vertex)
T_{opt}^*	Optimal temperature for photosynthesis (i.e., position of the parabola vertex) at full acclimation
$\tilde{T}_{opt}$	Shifted optimal temperature for photosynthesis ($\tilde{T}_{opt} = T_{opt} - a_{opt}\mu_T - b_{opt}$)
$\Delta T_{80\%}$	Width of the leaf temperature range for which $A_{net} \geq rA_{opt}$, with $r = 0.8$
$\Delta T_{80\%}^*$	Width of the leaf temperature range for which $A_{net} \geq rA_{opt}$, with $r = 0.8$, at full acclimation
α	'Size' of the Gaussian white noise
$\mu_{A_{net}}$	Mean net CO_2 assimilation rate
μ_T	Long-term mean leaf temperature
$\sigma_{A_{net}}$	Standard deviation of net CO_2 assimilation rate
σ_T	Standard deviation of leaf temperature, $\sigma_T = \alpha\sqrt{\frac{\tau_l}{2}}$
τ_l	Characteristic time scale of the changes in leaf temperature (i.e., relaxation constant of the Ornstein-Uhlenbeck process)
τ_{opt}	Relaxation constant of the dynamics of T_{opt}, corresponding to the time required for the plant to react to a change in temperature and reach $1 - e^{-1}$ ≅63% of full acclimation to the new thermal conditions
$\xi_{gn}(t)$	Gaussian uncorrelated white noise

Table S4 Summary of cases explored in this contribution and SI equations reporting the pdf of A_{net}.

	Only T_{opt} acclimates	T_{opt} and $\Delta T_{80\%}$ acclimate	T_{opt}, $\Delta T_{80\%}$ and A_{opt} acclimate
Acclimation to long-term mean temperature (or no acclimation)	Eqn (3)-(4)	Analytical pdf of A_{net} obtainable, but not reported	Monte Carlo approach for the derived distribution, starting from the pdf of T_l (Eqn 2)
Acclimation with finite delay	Eqn (11)	Analytical pdf of A_{net} obtainable, but not reported	Monte Carlo approach for the derived distribution, starting from the joint pdf of T_l and T_{opt} (Eqn 10)
Instantaneous acclimation	Eqn (5)-(6)	Analytical pdf of A_{net} obtainable, but not reported	Monte Carlo approach for the derived distribution, starting from the pdf of T_l (Eqn 2)

SI2.1 Leaf temperature dynamics as an Ornstein-Uhlenbeck process

The first step in the derivation of the pdf of A_{net} is the definition of the statistical properties of T_l. The temporal dynamics of T_l can be formalized via the following stochastic differential equation

$$\frac{dT_l(t)}{dt} = -\frac{T_l(t) - \mu_T}{\tau_l} + \alpha\xi_{gn}(t), \tag{1}$$

where $\xi_{gn}(t)$ is a Gaussian uncorrelated (i.e., white) noise, which is characterized by vanishing mean (i.e., $\langle\xi_{gn}(t)\rangle = 0$) and an autocorrelation function with a sharp peak in zero and an instantaneous drop to zero for larger time lags (i.e., $\langle\xi_{gn}(t)\,\xi_{gn}(t')\rangle = \delta(t - t')$)); α is the square root of the variations of the white noise (also referred to as noise 'size'); ${\tau_l}^{-1} > 0$ is the mean-reversion rate of the process (i.e., τ_l is the relaxation time); and μ_T is the long-term mean T_l. This approach to describe the dynamics of T_l has been previously adopted to describe air temperature by e.g., Benth and Šaltytė-Benth (2007). It is assumed that the same model also captures fluctuations in leaf temperature, on the ground of the (partial) coupling of leaf and air temperatures. With these assumptions, the random variable T_l has a steady-state Gaussian probability distribution, with mean μ_T and standard deviation $\sigma_T = \alpha\sqrt{\frac{\tau_l}{2}}$ (Gardiner, 1990), i.e.,

$$p(T_l) = \frac{1}{\sigma_T\sqrt{2\pi}}e^{-\frac{(T_l-\mu_T)^2}{2{\sigma_T}^2}} \tag{2}$$

SI2.2 Distribution of net CO_2 assimilation rate in the simplest cases

SI2.2.1 No acclimation and acclimation to the long-term mean leaf temperature

In the absence of acclimation or when acclimation is slow (i.e., leaves acclimate to the long-term mean temperature μ_T), the parameters of the $A_{net}(T_l)$ response curve do not follow the changes in T_l; rather, they are time-invariant. Under these conditions, T_{opt}, $\Delta T_{80\%}$, and A_{opt} can be treated as constant parameters or assumed to only vary with the long-term mean temperature μ_T. The derived distribution technique can be used to obtain $p_{long}(A_{net})$, starting from $p(T_l)$ (Eqn (2)) and considering the response curve $A_{net}(T_l)$. Because the parameters of $A_{net}(T_l)$ are independent of T_l, the $A_{net}(T_l)$ function can easily be inverted regardless of the type of acclimation observed. It is thus possible to obtain analytically $p_{long}(A_{net})$ (including the case of also $\Delta T_{80\%}$ changing with μ_T). The shape of the response of A_{net} to T_l is such that the resulting pdf comprises a continuous part and two atoms of probability, in $-R_{d,min}$ and $-R_{d,max}$ respectively. When only T_{opt} acclimates, the continuous part reads

$$p_{long,c}(A_{net}) = \frac{\Delta T_{80\%}}{4\sigma_T\sqrt{2\pi\left(A_{opt}-A_{net}\right)A_{opt}(1-r)}} \exp\left[-\frac{\left(1-\frac{A_{net}}{A_{opt}}\right)\Delta T_{80\%}{}^2 + 4(1-r)\left(\mu_T - T_{opt}\right)^2}{4(1-r)\sigma_T{}^2}\right] \left\{\exp\left[\left(-\frac{\mu_T - T_{opt}}{\sigma_T\sqrt{2}} + \frac{\Delta T_{80\%}}{2\sigma_T\sqrt{2}}\sqrt{\frac{A_{opt}-A_{net}}{A_{opt}(1-r)}}\right)^2\right] + \exp\left[\left(\frac{\mu_T - T_{opt}}{\sigma_T\sqrt{2}} + \frac{\Delta T_{80\%}}{2\sigma_T\sqrt{2}}\sqrt{\frac{A_{opt}-A_{net}}{A_{opt}(1-r)}}\right)^2\right]\right\}. \quad (3)$$

The two atoms of probability have mass

$$p_{0,low,long} = \int_{-\infty}^{T_{min}} p_{T_l}(T_l)dT_l = \frac{1}{2} - \frac{1}{2}\mathrm{erf}\left(\frac{\mu_T - T_{opt}}{\sigma_T\sqrt{2}} - \frac{\Delta T_{80\%}}{2\sigma_T}\sqrt{\frac{A_{opt}+R_{d,min}}{2A_{opt}(1-r)}}\right)$$
$$p_{0,high,long} = \int_{T_{max}}^{\infty} p_{T_l}(T_l)dT_l = \frac{1}{2} + \frac{1}{2}\mathrm{erf}\left(\frac{\mu_T - T_{opt}}{\sigma_T\sqrt{2}} - \frac{\Delta T_{80\%}}{2\sigma_T}\sqrt{\frac{A_{opt}+R_{d,max}}{2A_{opt}(1-r)}}\right) \quad (4)$$

where erf(·) is the error function, $T_{min,long} = T_{opt} - \frac{\Delta T_{80\%}}{2}\sqrt{\frac{A_{opt}+R_{d,min}}{A_{opt}(1-r)}}$, and

$T_{max,long} = T_{opt} + \frac{\Delta T_{80\%}}{2}\sqrt{\frac{A_{opt}+R_{d,max}}{A_{opt}(1-r)}}$. These quantities represent the probabilities that A_{net} equals $-R_{d,min}$ and $-R_{d,max}$ respectively.

SI2.2.2 Instantaneous acclimation

The derived distribution technique allows also determining the pdf of A_{net} in the extreme case of instantaneous acclimation, i.e., $p_{inst}(A_{net})$. If A_{opt} acclimates (alone or in conjunction with T_{opt} and/or $\Delta T_{80\%}$), a Monte Carlo approach is required to extract normally distributed T_l and calculate the corresponding A_{net}. The sample mean and standard deviation, and the frequency of $A_{net} \geq 0.8A_{opt}$ are then estimates of the performance metrics.

Conversely, when acclimation results in a change of T_{opt} (and/or $\Delta T_{80\%}$) while A_{opt} remains constant, $p_{inst}(A_{net})$ can be analytically obtained. Here the resulting formulas are reported only for the case of constant $\Delta T_{80\%}$, to avoid cumbersome formulations. The change in T_{opt} with temperature is described as $T_{opt} = a_{opt}T_l + b_{opt}$. This additional temperature effect makes the parabolic dependence $A_{net}(T_l)$ more complicated, but the approach employed for the case of no acclimation is still applicable. Hence, applying the derived distribution technique yields

$$p_{inst,c}(A_{net}) = \frac{\Delta T_{80\%}}{4\sigma_T\sqrt{2\pi\left(1-a_{opt}\right)^2\left(A_{opt}-A_{net}\right)A_{opt}(1-r)}} \exp\left[\frac{\Delta T_{80\%}(A_{net}+1)}{4A_{opt}\left(1-a_{opt}\right)^2(1-r){\sigma_T}^2} + \frac{\left(b_{opt}-\left(1-a_{opt}\right)\mu_T\right)^2}{\left(1-a_{opt}\right)^2{\sigma_T}^2}\right] \left\{\exp\left[\left(-\frac{b_{opt}+\left(a_{opt}-1\right)\mu_T}{\sqrt{2}\left(a_{opt}-1\right)\sigma_T} + \frac{\Delta T_{80\%}}{2\sigma_T\sqrt{2}}\sqrt{\frac{A_{opt}-A_{net}}{\left(1-a_{opt}\right)^2(1-r)}}\right)^2\right] + \exp\left[\left(\frac{b_{opt}+\left(a_{opt}-1\right)\mu_T}{\sqrt{2}\left(a_{opt}-1\right)\sigma_T} + \frac{\Delta T_{80\%}}{2\sigma_T\sqrt{2}}\sqrt{\frac{A_{opt}-A_{net}}{\left(1-a_{opt}\right)^2(1-r)}}\right)^2\right]\right\} \quad (5)$$

for the continuous part of the distribution. Also in this case there are the two atoms of probability, in $-R_{d,min}$ and $-R_{d,max}$ respectively:

$$p_{0,low,inst} = \int_{-\infty}^{T_{min,inst}} p_{T_l}(T_l)dT_l = \frac{1}{2} - \frac{1}{2}\mathrm{erf}\left(\frac{\mu_T - T_{min,inst}}{\sigma_T\sqrt{2}}\right)$$
$$p_{0,high,inst} = \int_{T_{max,inst}}^{\infty} p_{T_l}(T_l)dT_l = \frac{1}{2} + \frac{1}{2}\mathrm{erf}\left(\frac{\mu_T - T_{max,inst}}{\sigma_T\sqrt{2}}\right) \quad (6)$$

with $T_{min,inst} = -\frac{b_{opt}}{a_{opt}-1} - \frac{\Delta T_{80\%}}{2}\sqrt{\frac{A_{opt}+R_{d,min}}{A_{opt}(1-r)(a_{opt}-1)^2}}$ and $T_{max,inst} = -\frac{b_{opt}}{a_{opt}-1} + \frac{\Delta T_{80\%}}{2}\sqrt{\frac{A_{opt}+R_{d,max}}{A_{opt}(1-r)(a_{opt}-1)^2}}$.

SI2.3 Coupled dynamics of leaf temperature and acclimation parameters as a bi-dimensional Ornstein-Uhlenbeck process

Empirical results suggest that leaf net assimilation rate acclimates to the thermal environment and that the acclimation process occurs with a delay (Section S1.2). This is a more general (and realistic) case than those explored above that assume no acclimation, acclimation only to the long-term mean temperature (both cases in Section S2.2.1) or, at the other end of the spectrum, instantaneous acclimation (Section S2.2.2). Addressing the case of delayed acclimation requires describing the coupled dynamics of T_l and the acclimation parameters. The literature data suggest that most species acclimate (at least) by increasing T_{opt}, while the changes in $\Delta T_{80\%}$ and A_{opt} are less consistent (Figure S1, left). For these reasons, here the focus is on the coupled dynamics of T_l and T_{opt}, and then consider the changes in $\Delta T_{80\%}$ and A_{opt} as following those of T_{opt}. To quantify the implications of a finite delay in acclimation, it is assumed that T_{opt} acclimates to T_l according to a linear model, with a relaxation time (or delay), τ_{opt}, and an asymptotic value T^*_{opt} (Dietze (2014), Säll and Pettersson (1994); a similar model was used by Friend (2010) to describe the acclimation of the optimal temperature for electron transport rate). Here, T^*_{opt} corresponds to complete acclimation to the current T_l, i.e., $T^*_{opt} = a_{opt}T_l + b_{opt}$. In this model, T_{opt} tends exponentially to T^*_{opt}; the speed of change of T_{opt}, $\frac{dT_{opt}}{dt}$, depends on the distance of T_{opt} from T^*_{opt} and the relaxation time τ_{opt}, representing the time interval needed for T_{opt} to cover $1 - e^{-1} \cong$63% of the difference $T^*_{opt} - T_{opt}$. Thus, in general the instantaneous T_{opt} does not reach T^*_{opt} because acclimation is inherently slow ($\tau_{opt} > 0$) and T_l (and hence T^*_{opt}) change.

To describe a delayed acclimation, the dynamics of T_{opt} needs to be coupled to that of T_l, through its effect on T_{opt}^*. This can be expressed via the following coupled differential equations

$$\begin{cases} \dfrac{dT_l(t)}{dt} = -\dfrac{T_l(t) - \mu_T}{\tau_l} + \alpha\xi_{gn}(t) \\ \dfrac{dT_{opt}(t)}{dt} = \dfrac{T_{opt}^*\big(T_l(t)\big) - T_{opt}(t)}{\tau_{opt}} \end{cases}, \tag{7}$$

where the first equation represents the stochastic dynamics of T_l (as in Eqn (1)) and the second one describes the actual acclimation process (i.e., the dynamic link between optimal leaf temperature for photosynthesis, T_{opt}, and the current leaf temperature, T_l). There, $T_{opt}^* = a_{opt}T_l + b_{opt}$. The dynamics described by (7) is a bi-dimensional Ornstein-Uhlenbeck process (Gardiner, 1990). The joint probability density function of the variables T_l and T_{opt}, $p_{OU}(T_l, T_{opt})$ (where the subscript OU refers to the Ornstein-Uhlenbeck process), can be obtained analytically, as described next.

First, the system of equations (7) is recast as a function of the shifted variables $\widetilde{T_l} = T_l - \mu_T$ and $\tilde{T}_{opt} = T_{opt} - a_{opt}\mu_T - b_{opt}$. Following Gardiner (1990), it is possible to write the partial differential equation that describes the time evolution of $p_{OU}\big(\widetilde{T_l}, \tilde{T}_{opt}\big)$ (i.e., the Fokker Planck equation corresponding to Eqn (7)). Under stochastic steady state conditions, this equation reads

$$\frac{1}{2}\alpha^2 \frac{\partial^2 p_{OU}\big(\widetilde{T_l}, \tilde{T}_{opt}\big)}{\partial \widetilde{T_l}^2} + \frac{\widetilde{T_l}}{\tau_l}\frac{\partial p_{OU}\big(\widetilde{T_l}, \tilde{T}_{opt}\big)}{\partial \widetilde{T_l}} + \frac{1}{\tau_{opt}}\big(\tilde{T}_{opt} - a\widetilde{T_l}\big)\frac{\partial p_{OU}\big(\widetilde{T_l}, \tilde{T}_{opt}\big)}{\partial \tilde{T}_{opt}} + \left(\frac{1}{\tau_l} + \frac{1}{\tau_{opt}}\right) p_{OU}\big(\widetilde{T_l}, \tilde{T}_{opt}\big) = 0, \tag{8}$$

where $p_{OU}\big(\widetilde{T_l}, \tilde{T}_{opt}\big)$ is the steady state joint probability distribution of the shifted variables, $\widetilde{T_l}$ and $\tilde{T}_{opt}$. Solving this differential equation, $p_{OU}\big(\widetilde{T_l}, \tilde{T}_{opt}\big)$ is obtained as

$$p_{OU}\big(\widetilde{T_l}, \tilde{T}_{opt}\big) = \frac{\tau_l + \tau_{opt}}{a_{opt}\tau_l \pi \alpha^2}\sqrt{\frac{1}{\tau_l \tau_{opt}}}\exp\left\{-\frac{\tau_l + \tau_{opt}}{\alpha^2 \tau_l \tau_{opt}}\left[\widetilde{T_l}^2 + \frac{\tau_l + \tau_{opt}}{a_{opt}^2 \tau_l}\tilde{T}_{opt}^{\ 2} - \frac{2}{a_{opt}}\widetilde{T_l}\tilde{T}_{opt}\right]\right\}. \tag{9}$$

The joint distribution of the original variables, $p_{OU}(T_l, T_{opt})$, can be obtained as a bivariate derived distribution from (9), as $p_{OU}(T_l, T_{opt}) = J^{-1} p_{OU}\big(\widetilde{T_l}, \tilde{T}_{opt}\big)$, where J is the Jacobian of

the transformation of variables (Kottegoda & Rosso, 1998). Because the transformation from the shifted to the original variables is linear and has Jacobian equal to one, the distribution $p_{OU}(T_l, T_{opt})$ has the same shape of (9), but with different variables, i.e.,

$$p_{OU}(T_l, T_{opt}) = \frac{\tau_l + \gamma\tau_{opt}}{a_{opt}\tau_l \pi \alpha^2}\sqrt{\frac{1}{\tau_l \tau_{opt}}}\exp\left\{-\frac{\tau_l+\tau_{opt}}{\alpha^2\tau_l\tau_{opt}}\left[(T_l-\mu_T)^2 + \frac{\tau_l+\tau_{opt}}{a_{opt}^2\tau_l}\left(T_{opt} - a_{opt}\mu_T - b_{opt}\right)^2 - \frac{2}{a_{opt}}(T_l-\mu_T)\left(T_{opt}-a_{opt}\mu_T-b_{opt}\right)\right]\right\}. \quad (10)$$

The limit cases of $\tau_{opt} \to \infty$ and $\tau_{opt} \to 0$ correspond to the extreme cases of constant T_{opt} and instantaneous acclimation, respectively (Sections S2.2.1 and S2.2.2). Hence, the model assuming a finite acclimation delay represents a generalized description of the acclimation dynamics and includes the limiting cases presented in the previous sections.

SI2.4 Distribution of net CO_2 assimilation rate, with delayed acclimation

Knowledge of $p_{OU}(T_l, T_{opt})$ allows obtaining the joint distribution of A_{net} and T_{opt}, denoted as $p_{OU}(A_{net}, T_{opt})$, by accounting for the dependence of A_{net} on T_l and T_{opt}, and, through T_{opt}, on $\Delta T_{80\%}$ and A_{opt}(Eqn 1 in the main text). This step exploits again the derived distribution technique. The desired probability density function of A_{net}, $p_{OU}(A_{net})$, can be obtained as the marginal distribution of $p_{OU}(A_{net}, T_{opt})$ (i.e., integrating the joint distribution over all T_{opt} values).

Similarly to the case of instantaneous acclimation, this approach is amenable to analytical solutions only if A_{opt} does not acclimate and the response curve $A_{net}(T_l)$ can be inverted analytically. Here the solution for the simplest case, in which only T_{opt} acclimates, is reported. The continuous part of the pdf of A_{net} reads

$$p_{OU}(A_{net}) = \int_{-\infty}^{\infty} p_{OU}(A_{net}, T_{opt})\ dT_{opt} =$$

$$= \frac{\Delta T_{80\%}\sqrt{\tau_l + \tau_{opt}}}{4\alpha\tau_l\sqrt{\pi A_{opt}\left(A_{opt}-A_{net}\right)(1-r)\left(1-2a_{opt}+{a_{opt}}^2+\frac{\tau_{opt}}{\tau_l}\right)}}\left\{\exp\left[c_{1,+}-\frac{c_{2,+}}{c_3}\right]+\exp\left[c_{1,-}-\frac{c_{2,-}}{c_3}\right]\right\}, \quad (11)$$

where for notational simplicity the coefficients $c_{1,\mp}$, $c_{2,\mp}$, and c_3 are defined as

$$c_{1,\mp} = c_4\left[\frac{\mu_T}{\tau_l}\left(\frac{2b_{opt}}{a_{opt}} - \mu_T\right) - \frac{{b_{opt}}^2(\tau_l + \tau_{opt})}{{a_{opt}}^2\tau_l\tau_{opt}} - \frac{{\Delta T_{80\%}}^2}{4(1-r)\tau_{opt}}\left(1 - \frac{A_{net}}{A_{opt}}\right)\right] \mp b_{opt}c_5$$

$$c_{2,\mp} = \left\{\frac{2}{a_{opt}}c_4\left[\frac{\mu_T}{\tau_l} - \frac{b_{opt}}{\tau_{opt}} + \frac{b_{opt}(\tau_l + \tau_{opt})}{a_{opt}\tau_l\tau_{opt}}\right] \mp (a_{opt} - 1)c_5\right\}^2 \qquad (12)$$

$$c_3 = \frac{c_4}{\tau_{opt}}\left[\frac{2}{a_{opt}} - \frac{\tau_l + \tau_{opt}}{{a_{opt}}^2\tau_l} - 1\right],$$

with c_4, and c_5 given by

$$c_4 = \frac{\tau_l + \tau_{opt}}{\alpha^2\tau_l}$$

$$c_5 = -\frac{\Delta T_{80\%}(\tau_l + \tau_{opt})}{\alpha^2 a_{opt}\tau_l\tau_{opt}}\sqrt{\frac{A_{opt} - A_{net}}{A_{opt}(1-r)}}. \qquad (13)$$

The atoms of probability have mass

$$p_{0,low,OU} = \int_{-\infty}^{+\infty}\int_{-\infty}^{T_{min}} p_{OU}(T_l, T_{opt})dT_l\, dT_{opt}$$

$$p_{0,high,OU} = \int_{-\infty}^{+\infty}\int_{T_{max}}^{\infty} p_{OU}(T_l, T_{opt})dT_l\, dT_{opt} \qquad (14)$$

where $T_{min,OU} = T_{opt} - \frac{\Delta T_{80\%}}{2}\sqrt{\frac{A_{opt}+R_{d,min}}{A_{opt}(1-r)}}$ and $T_{max,OU} = T_{opt} + \frac{\Delta T_{80\%}}{2}\sqrt{\frac{A_{opt}+R_{d,max}}{A_{opt}(1-r)}}$.

In the most general case of A_{opt} and $\Delta T_{80\%}$ covarying with T_{opt} as a result of acclimation, the above approach is not applicable, because the parabolic dependence $A_{net}(T_l)$ cannot be inverted. Nevertheless, knowledge of the joint distribution of T_l and T_{opt} (and their marginal and conditional distributions) allows employing nested conditioning to generate vectors of T_l and T_{opt} with the desired distributions and covariance (Lemieux, 2009). Specifically, from the joint distribution $p_{OU}(T_l, T_{opt})$ (Eqn (10)), the marginal distribution of T_l, $p_{OU,T_l}(T_l)$ and its cumulative distribution function (cdf), $P_{OU,T_l}(T_l)$, are determined. It is also possible to obtain the conditional pdf of T_{opt} given T_l, $p_{OU,T_{opt}|T_l}(T_{opt}|T_l) = p_{OU}(T_l, T_{opt})\, p_{OU,T_l}(T_l)^{-1}$, and the corresponding cdf, $P_{OU,T_{opt}|T_l}(T_{opt}|T_l)$. Pairs of T_l and T_{opt} with joint distribution $p_{OU}(T_l, T_{opt})$ are generated by sampling uniform distributions over [0,1] corresponding to pairs of $\left\{P_{OU,T_l}(T_l)^*, P_{OU,T_{opt}|T_l}(T_{opt}|T_l)^*\right\}$ and inverting the two cdfs. The generated pairs of T_l and T_{opt} are used to determine A_{net} based on the dependence $A_{net}(T_l)$ (Eqn 1 in the main text). The performance metrics can then be readily calculated as sample mean, standard deviation and fraction of cases where $A_{net} \geq 0.8A_{opt}$. It should be noted that in this case

A_{net} is neither upper nor lower bounded, as also $-R_{d,min}$ and $-R_{d,max}$ change with acclimating A_{opt}. Hence no atom of probability emerges.

SI3- Supplementary results

Figure S4 complements the results summarized in Figure 3 and 4 in the main text, by reporting the leaf performance proxies for three selected species that acclimate by reducing T^*_{opt}. Among these species, the most common response is an increase in $\Delta T^*_{80\%}$ and decrease in A^*_{opt}, as in *Phaseolus vulgaris* (Figure S4, top row), followed by the case of both $\Delta T^*_{80\%}$ and A^*_{opt} increasing with T_{growth} (e.g., *Plantago euryphylla*; middle row). In *Chenopodium album* (bottom row), acclimation reduces T^*_{opt}, $\Delta T^*_{80\%}$ and A^*_{opt}. The general patterns are similar to those emerging for species that acclimate by increasing T^*_{opt} (Figure 4 in the main text), although the reduction of T^*_{opt} with increasing T_l narrows the range of mean temperatures where the performance is high and stable, in particular towards higher mean temperatures.

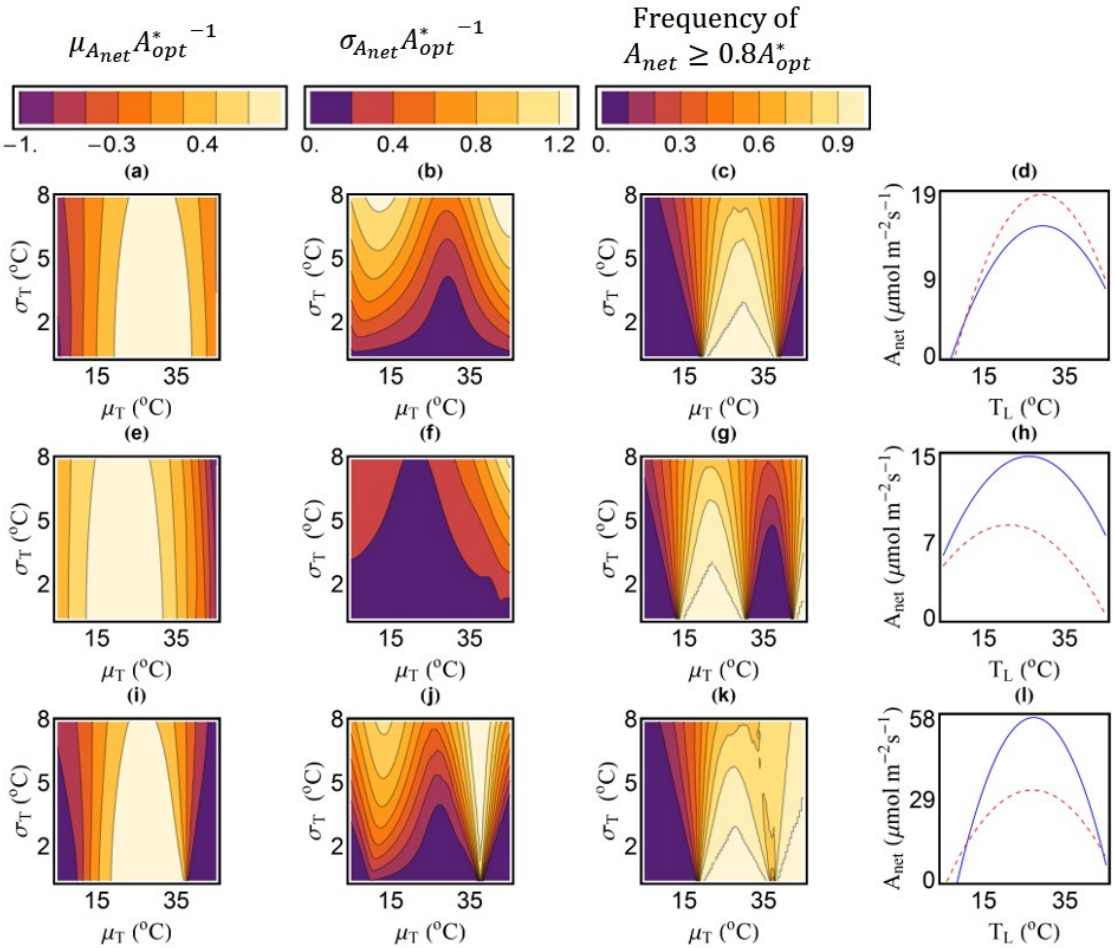

Figure S4 Effects on plant performance of a shift in the leaf thermal regime for three selected species with different acclimation strategies: *Phaseolus vulgaris* (top, panels (a)-(d)), *Plantago euryphylla* (middle, panels (e)-(h)) and *Chenopodium album* (bottom, panels (i)-(l)). The leaf thermal regime is summarized by the long-term average leaf temperature, μ_T (x-axis) and its standard deviation, σ_T (y-axis). Plant performance is summarized by mean (left column) and standard deviation (second column) of A_{net}, both normalized by the species- and condition-specific A_{opt}; and fraction of time spent under optimal or near-optimal condition (third column). To facilitate the comparison across species, a single color map is used throughout each column, and reported at its bottom. For each species, the $A_{net}(T_l)$ curves for two of the experimental temperatures are reported in the far right column, where blue solid lines refer to the lowest and red dashed lines to the highest temperature considered in each experiment. The species-specific parameters are summarized in Table S2. As in the main text, $\tau_l = \tau_{opt} = 10$ days.

References

Aspinwall M.J., Varhammar A., Blackman C.J., Tjoelker M.G., Ahrens C., Byrne M., . . . Rymer P.D. (2017) Adaptation and acclimation both influence photosynthetic and respiratory temperature responses in Corymbia calophylla. *Tree physiology*, **37**, 1095-1112.

Atkin O.K., Scheurwater I. & Pons T.L. (2006) High thermal acclimation potential of both photosynthesis and respiration in two lowland *Plantago* species in contrast to an alpine congeneric. *Global Change Biology*, **12**, 500-515.

Atkin O.K., Scheurwater I. & Pons T.L. (2007) Respiration as a percentage of daily photosynthesis in whole plants is homeostatic at moderate, but not high, growth temperatures. *New Phytologist*, **174**, 367-380.

Badger M.R., Björkman O. & Armond P.A. (1982) An analysis of photosynthetic response and adaptation to temperature in higher plants: temperature acclimation in the desert evergreen Nerium oleander L*. *Plant, Cell & Environment*, **5**, 85-99.

Battaglia M., Beadle C. & Loughhead S. (1996) Photosynthetic temperature responses of *Eucalyptus globulus* and *Eucalyptus nitens*. *Tree Physiology*, **16**, 81-89.

Benth F.E. & Šaltytė-Benth J. (2007) The volatility of temperature and pricing of weather derivatives. *Quantitative Finance*, **7**, 553-561.

Berry J. & Bjorkman O. (1980) Photosynthetic response and adaptation to temperature in higher plants. *Annual Review of Plant Physiology and Plant Molecular Biology*, **31**, 491-543.

Billings W.D., Godfrey P.J., Chabot B.F. & Bourque D.P. (1971) Metabolic acclimation to temperature in arctic and alpine ecotypes of *Oxyria digyna*. *Arctic and Alpine Research*, **3**, 277-289.

Björkman O., Badger M.R. & Armond P.A. (1978) Thermal acclimation of photosynthesis: effect of growth temperature on photosynthetic characteristics and components of the photosynthetic apparatus in *Nerium oleander*. *Carnegie Institute Washington Yearbook*, **77**, 262-282.

Björkman O. & Pearcy R.W. (1971) Effects of growth temperature dependence of photosynthesis in vivo and CO_2 fixation by carboxydismutase in vitro in C3 and C4 species. *Carnegie Institute Washington Yearbook*, **70**, 511-520.

Bunce J.A. (2000) Acclimation of photosynthesis to temperature in eight cool and warm climate herbaceous C3 species: Temperature dependence of parameters of a biochemical photosynthesis model. *Photosynthesis Research*, **63**, 59-67.

Bunce J.A. (2008) Acclimation of photosynthesis to temperature in *Arabidopsis thaliana* and *Brassica oleracea*. *Photosynthetica*, **46**, 517-524.

Cowling S.A. & Sage R.F. (1998) Interactive effects of low atmospheric CO_2 and elevated temperature on growth, photosynthesis and respiration in *Phaseolus vulgaris*. *Plant, Cell & Environment*, **21**, 427-435.

Cunningham S.C. & Read J. (2002) Comparison of temperate and tropical rainforest tree species: photosynthetic responses to growth temperature. *Oecologia*, **133**, 112-119.

Dahal K., Kane K., Gadapati W., Webb E., Savitch L.V., Singh J., . . . Hüner N.P.A. (2012) The effects of phenotypic plasticity on photosynthetic performance in winter rye, winter wheat and *Brassica napus*. *Physiologia Plantarum*, **144**, 169-188.

Dietze M.C. (2014) Gaps in knowledge and data driving uncertainty in models of photosynthesis. *Photosynthesis Research*, **119**, 3-14.

Downton J. & Slatyer R.O. (1972) Temperature dependence of photosynthesis in cotton. *Plant Physiology*, **50**, 518-522.

Dwyer S.A., Ghannoum O., Nicotra A. & Von Caemmerer S. (2007) High temperature acclimation of C4 photosynthesis is linked to changes in photosynthetic biochemistry. *Plant, Cell & Environment*, **30**, 53-66.

Ferrar P., Slatyer R. & Vranjic J. (1989) Photosynthetic temperature acclimation in *Eucalyptus* species from diverse habitats, and a comparison with *Nerium oleander*. *Functional Plant Biology*, **16**, 199-217.

Forseth I. & Ehleringer J. (1982) Ecophysiology of two solar-tracking desert winter annuals. I. Photosynthetic acclimation to growth temperature. *Functional Plant Biology*, **9**, 321-332.

Friend A.D. (2010) Terrestrial plant production and climate change. *Journal of Experimental Botany*, **61**, 1293-1309.

Gandin A., Koteyeva N.K., Voznesenskaya E.V., Edwards G.E. & Cousins A.B. (2014) The acclimation of photosynthesis and respiration to temperature in the C-3-C-4 intermediate Salsola divaricata: induction of high respiratory CO_2 release under low temperature. *Plant Cell and Environment*, **37**, 2601-2612.

Gardiner G.W. (1990) *Handbook of stochastic methods for physics, chemistry and the natural sciences*. (2nd ed.). Springer, Berlin.

Ghannoum O., Phillips N.G., Conroy J.P., Smith R.A., Attard R.D., Woodfield R., . . . Tissue D.T. (2010) Exposure to preindustrial, current and future atmospheric CO_2 and temperature differentially affects growth and photosynthesis in *Eucalyptus*. *Global Change Biology*, **16**, 303-319.

Graves J.D. & Taylor K. (1988) A comparative study of *Geum rivale* L. and *G. urbanum* L. to determine those factors controlling their altitudinal distribution. II. Photosynthesis and respiration. *The New Phytologist*, **108**, 297-304.

Gunderson C.A., Norby R.J. & Wullschleger S.D. (2000) Acclimation of photosynthesis and respiration to simulated climatic warming in northern and southern populations of *Acer saccharum*: laboratory and field evidence. *Tree Physiology*, **20**, 87-96.

Haldimann P. & Feller U. (2005) Growth at moderately elevated temperature alters the physiological response of the photosynthetic apparatus to heat stress in pea (Pisum sativum L.) leaves. *Plant, Cell & Environment*, **28**, 302-317.

Hill R.S., Read J. & Busby J.R. (1988) The temperature-dependence of photosynthesis of some Australian temperate rainforest trees and its biogeographical significance. *Journal of Biogeography*, **15**, 431-449.

Ishikawa K., Onoda Y. & Hikosaka K. (2007) Intraspecific variation in temperature dependence of gas exchange characteristics among *Plantago asiatica* ecotypes from different temperature regimes. *The New Phytologist*, **176**, 356-364.

Kemp P.R. & Williams G.J. (1980) A physiological basis for niche separation between *Agropyron smithii* (C3) and *Bouteloua gracilis* (C4). *Ecology*, **61**, 846-858.

Kositsup B., Montpied P., Kasemsap P., Thaler P., Améglio T. & Dreyer E. (2009) Photosynthetic capacity and temperature responses of photosynthesis of rubber trees (*Hevea brasiliensis* Müll. Arg.) acclimate to changes in ambient temperatures. *Trees*, **23**, 357-365.

Kottegoda N.T. & Rosso (1998) *Statistics, probability and reliability for civil and environmental engineers*. McGraw-Hill, New York.

Kruse J., Adams M.A., Kadinov G., Arab L., Kreuzwieser J., Alfarraj S., . . . Rennenberg H. (2017) Characterization of photosynthetic acclimation in *Phoenix dactylifera* by a modified Arrhenius equation originally developed for leaf respiration. *Trees-Structure and Function*, **31**, 623-644.

Kubien D.S. & Sage R.F. (2004) Low-temperature photosynthetic performance of a C4 grass and a co-occurring C3 grass native to high latitudes. *Plant, Cell & Environment*, **27**, 907-916.

Lemieux C. (2009) *Monte Carlo and quasi-Monte Carlo sampling*. Springer.

Lorenz H.P. & Wiebe H.J. (1980) Effect of temperature on photosynthesis of lettuce adapted to different light and temperature conditions. *Scientia Horticulturae*, **13**, 115-123.

Massacci A., Iannelli M.A., Pietrini F. & Loreto F. (1995) The effect of growth at low temperature on photosynthetic characteristics and mechanisms of photoprotection of maize leaves. *Journal of Experimental Botany*, **46**, 119-127.

Mawson B.T., Svoboda J. & Cummins R.W. (1986) Thermal acclimation of photosynthesis by the arctic plant *Saxifraga cernua*. *Canadian Journal of Botany*, **64**, 71-76.

Monson R.K., Jaeger C.H., Adams W.W., Driggers E.M., Silver G.M. & Fall R. (1992) Relationships among isoprene emission rate, photosynthesis, and isoprene synthase activity as influenced by temperature. *Plant Physiology*, **98**, 1175-1180.

Monson R.K., Robert O. Littlejohn, Jr. & Williams G.J. (1983) Photosynthetic adaptation to temperature in four species from the Colorado shortgrass steppe: A physiological model for coexistence. *Oecologia*, **58**, 43-51.

Mooney H.A. (1980) Photosynthetic plasticity of populations of *Heliotropium curassavicum* L. originating from differing thermal regimes. *Oecologia*, **45**, 372-376.

Mooney H.A., Björkman O. & Collatz G.J. (1978) Photosynthetic acclimation to temperature in the desert shrub, *Larrea divaricata* I. Carbon Dioxide Exchange Characteristics of Intact Leaves. *Plant Physiology*, **61**, 406-410.

Nagai T. & Makino A. (2009) Differences between rice and wheat in temperature responses of photosynthesis and plant growth. *Plant and Cell Physiology*, **50**, 744-755.

Naidu S.L., Moose S.P., AL-Shoaibi A.K., Raines C.A. & Long S.P. (2003) Cold tolerance of C_4 photosynthesis in *Miscanthus* × giganteus: Adaptation in mmounts and sequence of C_4 photosynthetic enzymes. *Plant Physiology*, **132**, 1688-1697.

Neilson R.E., Ludlow M.M. & Jarvis P.G. (1972) Photosynthesis in sitka spruce (*Picea sitchensis* (Bong.) Carr.). II. Response to temperature. *Journal of Applied Ecology*, **9**, 721-745.

Ngugi M.R., Hunt M.A., Doley D., Ryan P. & Dart P.J. (2003) Photosynthetic light and temperature responses of *Eucalyptus cloeziana* and *Eucalyptus argophloia*. *Australian Journal of Botany*, **51**, 573-583.

Nobel P.S. & Hartsock T.L. (1981) Shifts in the optimal temperature for nocturnal CO_2 uptake caused by changes in growth temperature for cacti and agaves. *Physiologia Plantarum*, **53**.

Paul M.J., Lawlor D.W. & Driscoll S.P. (1990) The effect of temperature on photosynthesis and carbon fluxes in sunflower and rape. *Journal of Experimental Botany*, **41**, 547-555.

Pearcy R.W. (1977) Acclimation of Photosynthetic and Respiratory Carbon Dioxide Exchange to Growth Temperature in Atriplex lentiformis (Torr.) Wats. *Plant Physiology*, **59**, 795-799.

Pearcy R.W., Tumosa N. & Williams K. (1981) Relationships between growth, photosynthesis and competitive interactions for a C_3 and a C_4 plant. *Oecologia*, **48**, 371-376.

Pittermann J. & Sage R.F. (2000) Photosynthetic performance at low temperature of Bouteloua gracilis Lag., a high-altitude C4 grass from the Rocky Mountains, USA. *Plant, Cell & Environment*, **23**, 811-823.

Pons T.L. (2012) Interaction of temperature and irradiance effects on photosynthetic acclimation in two accessions of *Arabidopsis thaliana*. *Photosynthesis Research*, **113**, 207-219.

Rasulov B., Bichele I., Hüve K., Vislap V. & Niinemets Ü. (2015) Acclimation of isoprene emission and photosynthesis to growth temperature in hybrid aspen: resolving structural and physiological controls. *Plant, Cell & Environment*, **38**, 751-766.

Read J. (1990) Some effects of acclimation temperature on net photosynthesis in some tropical and extra-topical Australasian *Nothofagus* species. *Journal of Ecology*, **78**, 100-112.

Read J. & Busby J.R. (1990) Comparative responses to temperature of the major canopy species of Tasmanian cool temperate rainforest and their ecological significance. II. Net photosynthesis and climate analysis. *Australian Journal of Botany*, **38**, 185-205.

Sage R.F., Santrucek J. & Grise D.J. (1995) Temperature effects on the photosynthetic response of C3 plants to long-term CO_2 enrichment. *Vegetatio*, **121**, 67-77.

Säll T. & Pettersson P. (1994) A model of photosynthetic acclimation as a special case of reaction norms. *Journal of Theoretical Biology*, **166**, 1-8.

Sayed O.H., Emes M.J., Earnshaw M.J. & Butler R.D. (1989) Photosynthetic responses of different varieties of wheat to high temperature: I. Effect of growth temperature on development and photosynthetic performance. *Journal of Experimental Botany*, **40**, 625-631.

Sendall K.M., Reich P.B., Zhao C.M., Hou J.H., Wei X.R., Stefanski A., . . . Montgomery R.A. (2015) Acclimation of photosynthetic temperature optima of temperate and boreal tree species in response to experimental forest warming. *Global Change Biology*, **21**, 1342-1357.

Sheu B.-H. & Lin C.-K. (1999) Photosynthetic response of seedlings of the sub-tropical tree *Schima superba* with exposure to elevated carbon dioxide and temperature. *Environmental and Experimental Botany*, **41**, 57-65.

Silim S.N., Ryan N. & Kubien D.S. (2010) Temperature responses of photosynthesis and respiration in *Populus balsamifera* L.: acclimation versus adaptation. *Photosynthesis Research*, **104**, 19-30.

Slatyer R. (1977a) Altitudinal variation in the photosynthetic characteristics of snow gum, *Eucalyptus pauciflora* Sieb. Ex Spreng. III. Temperature response of material grown in contrasting thermal environments. *Functional Plant Biology*, **4**, 301-312.

Slatyer R. (1977b) Altitudinal variation in the photosynthetic characteristics of snow gum, *Eucalyptus pauciflora* Sieb. ex Spreng. IV. Temperature response of four populations grown at different temperatures. *Functional Plant Biology*, **4**, 583-594.

Slatyer R. & Ferrar P. (1977) Altitudinal variation in the photosynthetic characteristics of snow gum, *Eucalyptus pauciflora* Sieb. ex Spreng. V. Rate of acclimation to an altered growth environment. *Functional Plant Biology*, **4**, 595-609.

Slayter R. (1977) Altitudinal variation in the photosynthetic characteristics of snow gum, *Eucalyptus pauciflora* Sieb. ex Spreng. IV. Temperature response of four populations grown at different temperatures. *Functional Plant Biology*, **4**, 583-594.

Slot M. & Winter K. (2017) Photosynthetic acclimation to warming in tropical forest tree seedlings. *Journal of Experimental Botany*, **68**, 2275-2284.

Smith E.M. & Hadley E.B. (1974) Photosynthetic and respiratory acclimation to temperature in *Ledum groenlandicum* populations. *Arctic and Alpine Research*, **6**, 13-27.

Teskey R.O. & Will R.E. (1999) Acclimation of loblolly pine (*Pinus taeda*) seedlings to high temperatures. *Tree Physiology*, **19**, 519-525.

Toft N.L. & Pearcy R.W. (1982) Gas exchange characteristics and temperature relations of two aesert Annuals: A Comparison of a winter-active and a summer-active species. *Oecologia*, **55**, 170-177.

Tranquillini W., Havranek W.M. & Ecker P. (1986) Effects of atmospheric humidity and acclimation temperature on the temperature response of photosynthesis in young Larix decidua Mill. *Tree Physiology*, **1**, 37-45.

Vallejos C.E. & Pearcy R.W. (1987) Differential acclimation potential to low temperatures in two species of *Lycopersicon:* photosynthesis and growth. *Canadian Journal of Botany*, **65**, 1303-1307.

Veres J.S. & Williams G.J. (1984) Time course of photosynthetic temperature acclimation in *Carex eleocharis* Bailey. *Plant, Cell & Environment*, **7**, 545-547.

Wardlaw I., Begg J., Bagnall D. & Dunstone R. (1983) Jojoba: Temperature adaptation as expressed in growth and leaf function. *Functional Plant Biology*, **10**, 299-312.

Warren C.R. (2008) Does growth temperature affect the temperature responses of photosynthesis and internal conductance to CO_2 A test with *Eucalyptus regnans*. *Tree Physiology*, **28**, 11-19.

Way D.A. & Sage R.F. (2008a) Elevated growth temperatures reduce the carbon gain of black spruce *[Picea mariana* (Mill.) B.S.P.]. *Global Change Biology*, **14**, 624-636.

Way D.A. & Sage R.F. (2008b) Thermal acclimation of photosynthesis in black spruce [*Picea mariana* (Mill.) B.S.P.]. *Plant, Cell & Environment*, **31**, 1250-1262.

Way D.A., Stinziano J.R., Berghoff H. & Oren R. (2017) How well do growing season dynamics of photosynthetic capacity correlate with leaf biochemistry and climate fluctuations? *Tree Physiology*, **37**, 879-888.

Way D.A. & Yamori W. (2014) Thermal acclimation of photosynthesis: on the importance of adjusting our definitions and accounting for thermal acclimation of respiration. *Photosynthesis Research*, **119**, 89-100.

Williams D.G. & Black R.A. (1993) Phenotypic variation in contrasting temperature environments: Growth and photosynthesis in *Pennisetum setaceum* from different altitudes on Hawaii. *Functional Ecology*, **7**, 623-633.

Williams G.J. (1974) Photosynthetic adaptation, to temperature in C3 and C4 Grasses - A Possible ecological role in the shortgrass prairie. *Plant Physiology*, **54**, 709-711.

Xiong F.S., Mueller E.C. & Day T.A. (2000) Photosynthetic and respiratory acclimation and growth response of Antarctic vascular plants to contrasting temperature regimes. *American Journal of Botany*, **87**, 700-710.

Yamasaki T., Yamakawa T., Yamane Y., Koike H., Satoh K. & Katoh S. (2002) Temperature acclimation of photosynthesis and related changes in photosystem II electron transport in winter wheat. *Plant Physiology*, **128**, 1087-1097.

Yamori W., Hikosaka K. & Way D.A. (2014) Temperature response of photosynthesis in C-3, C-4, and CAM plants: temperature acclimation and temperature adaptation. *Photosynthesis Research*, **119**, 101-117.

Yamori W., Noguchi K., Hanba Y.T. & Terashima I. (2006) Effects of Internal Conductance on the Temperature Dependence of the Photosynthetic Rate in Spinach Leaves from Contrasting Growth Temperatures. *Plant and Cell Physiology*, **47**, 1069-1080.

Yamori W., Noguchi K., Hikosaka K. & Terashima I. (2010) Phenotypic Plasticity in Photosynthetic Temperature Acclimation among Crop Species with Different Cold Tolerances. *Plant Physiology*, **152**, 388-399.

Yamori W., Noguchi K., Kashino Y. & Terashima I. (2008) The Role of Electron Transport in Determining the Temperature Dependence of the Photosynthetic Rate in Spinach Leaves Grown at Contrasting Temperatures. *Plant and Cell Physiology*, **49**, 583-591.

Yamori W., Noguchi K.O. & Terashima I. (2005) Temperature acclimation of photosynthesis in spinach leaves: analyses of photosynthetic components and temperature dependencies of photosynthetic partial reactions. *Plant, Cell & Environment*, **28**, 536-547.

Yamori W., Suzuki K., Noguchi K.O., Nakai M. & Terashima I. (2006) Effects of Rubisco kinetics and Rubisco activation state on the temperature dependence of the photosynthetic rate in spinach leaves from contrasting growth temperatures. *Plant, Cell & Environment*, **29**, 1659-1670.

Yamori W. & von Caemmerer S. (2009) Effect of Rubisco Activase Deficiency on the Temperature Response of CO_2 Assimilation Rate and Rubisco Activation State: Insights from Transgenic Tobacco with Reduced Amounts of Rubisco Activase. *Plant Physiology*, **151**, 2073-2082.

Zaka S., Frak E., Julier B., Gastal F. & Louarn G. (2016) Intraspecific variation in thermal acclimation of photosynthesis across a range of temperatures in a perennial crop. *AoB PLANTS*, **8**, plw035-plw035.

Zhang X.W., Wang J.R., Ji M.F., Milne R.I., Wang M.H., Liu J.-Q., . . . Zhao C.-M. (2015) Higher Thermal Acclimation Potential of Respiration but Not Photosynthesis in Two Alpine Picea Taxa in Contrast to Two Lowland Congeners. *PLOS ONE*, **10**, e0123248.

Ziska L.H. (2001) Growth temperature can alter the temperature dependent stimulation of photosynthesis by elevated carbon dioxide in Albutilon theophrasti. *Physiologia Plantarum*, **111**, 322-328.